Interactive comment on "Subglacial sediment transport upstream of a basal channel in the ice shelf of Support Force Glacier (West Antarctica), identified by reflection seismics" *by*

Coen Hofstede et al.

RC1:

Dear authors,

I really enjoyed reading your manuscript - I'm very sorry that it has taken me so long to review it.

Dear reviewers,

Many thanks for your input in helping improve this manuscript. My apologies for the delay, it took longer than I had expected. My answers to the points you raise are written in italic format.

Coen Hofstede

General comments:

We would like to adjust our interpretation: The off-nadir reflections probably come from the subglacial channel connecting to the basal channel. Through interaction with the warmer ocean the subglacial channel increases its when approaching the grounding line. In our answer to reviewer #2 we explain our adjusted interpretation elaborately.

General comments:
The paper explores a little-studied feature in the base of Antarctic ice shelves, but one that is nonetheless important for ice shelf stability and sub ice-shelf circulation. The study also indicates subglacial sediment transport. The data acquisition and processing is of a high standard and the imaging is unambiguous. Most of the comments in the attachment are suggestions for grammatical corrections or improvements for readability; some of the paragraphs seem a little rushed, and some sentences aren't as easily understood as I think they might be. I also have some more substantive requests for clarification of a few points, as mentioned below, but I don't think that these are major issues. Overall, I think that the paper is a nice contribution to the understanding of ice shelves and their dynamics.

Best regards, Adam Booth Specific comments:

Abstract - I found this a little qualitative, and maybe some hints at the dimensions of the subglacial channel could be useful?

Abstract: Agreed

P2 L7-8 - similar to my comment in the abstract, maybe some quantitative detail about the geometry of surface channels could be useful?

P2 L7-8: Agreed

P3 L12 - 'active source' seismic

P3 L12: Corrected

P3 L16 - if its important to mention the date of the radar acquisitions, do so for the seismic too; I'm not sure you say when the data were acquired at any point in the manuscript.

P3 L16: Agreed. Both the seismic and radar surveys took place in January 2020, the radar survey shortly after the seismic survey.

Figure 1. Add a distance scale for the arrow lengths in (a). I also wonder if the figure would benefit from some textual geographic labels (e.g., the landmarks and features mentioned in the intro?).

Figure 1: Agreed

Section 2.5 - again, I'd mention the acquisition date here.

Section 2.5: Agreed

P6 L3 - define p as compressional (equally, S as shear when it comes up later). Additionally, you occasionally swap between "P wave" and "p wave". Be consistent.

P6 L3: Agreed.

P6 L4 - your sample rate is actually a sample interval.

P6 L4: Indeed, thanks

P6 L5 - consider putting the manufacturer of the GEODE system... something like "four Geometrics GEODE units"?

P6 L5: Agreed

P6 L7 - should II be III, given the information in Table 1?

P6 L7 :Well spotted, thanks

P6 L10 - I think your description of the acquisition (particularly for the long offset gathers, but maybe also for the profiles) might benefit from a schematic diagram of the survey.

P6 L10: Although it does make the text more readable we refrained from this as they hardly play a role in the results and discussion.

P7 L9 - define R(theta) at the start of this paragraph, otherwise Reflectivity and the symbol in Equation (2) is undefined.

P7 L9: Thanks we will

P7 L11 - it's unclear how Vp, Vs and rho relate to the primary reflectivity, in the way that you have described it here. I would consider splitting this sentence, explaining how reflectivity is defined by contrasts in these quantities, and then introducing Equation (2).

P7 L11: You're right, we've built up this part differently now.

P7 L14 - just give the Section number explicitly, rather than the cumbersome "determination of A0 subsection".

P7 L14 : Agreed

P7 L20 - give references for the parameter ranges you use in Table 2, to provide you with reflectivity ranges.

P7 L20: Agreed

Table 2 - explicitly state which material would have subscript 1 and 2 (i.e., which is above and below the interface). You might also consider defining the impedances as well as the Reflection coefficients?

Table2: Agreed

P9 L15 - the abrupt transition is, of course, only abrupt on the wavelength scale of your wavelet; maybe simply adding "at the XX m scale of vertical resolution" in here?

P9 L15: Correct, based on the center frequency

P9 L19 - here, and throughout, I think you're mis-using the term 'accuracy'. If something has 19% accuracy then it is very poor indeed! Do you mean 19% uncertainty, or "accuracy better than 81%", or suchlike? If I'm correct, that you're mis-using this term, make sure that other instances of accuracy are checked too. In this specific case, it's also not clear to me how the numbers above end up giving this accuracy.

P9 L19 Thank you, indeed we mean uncertainty

Section 3.1, header - I'm not sure that these are 'artefacts' as such, which I'd consider more to be residual effects of processing (e.g., migration smiles). I'd suggest that this subsection is retitled "Seabed depth conversion"?

Section 3.1: Agreed, it is not an artefact. We'll use "Seabed-depth conversion".

Figure 2 - this is a nice figure, but I'd suggest that the other figures in the section are given the same interpretation panels - it's unclear why you'd only provide it for this one. It might also be good to show an enlarged section of the subglacial feature; I know it features in other figures, but I really couldn't see it here.

Figure 2: Yes we agree and will add the schematic versions. Regarding the subglacial feature, I think the raw shots give the best indication we are dealing with reflections and will add them here. Lastly, I'm glad you appreciate the lay-out of figure 2

Figure 2 caption - "switches from positive to negative" - how do you define what is positive and negative polarity? You might just be better saying "changes polarity".

Figure 2 caption: Agreed but now we define positive and negative polarity in the text

P11 L3 - it seems a little premature to be referring to this feature as a 'drainage' feature. It's only in the Discussion where you start to present the evidence for this, based on previous work. At the moment, it is a subglacial feature, but it's impossible to know it's a 'drainage' feature from the seismic results alone. I'd suggest that you remove 'drainage' at this point in the manuscript.

P11 L3: Yes we agree, we'd like to call this the''subglacial feature''

P11 L7-8 - is the gradational, rather than abrupt, transition the reason why you see the deviation to smaller-magnitude reflectivity? Is it worth making this comment explicitly?

P11 L7-8: Yes we think so, the loss must be greater at the gradual ice-seawater contact. We point this out in the discussion (page 20 L6-9) as a general comment, not restricted to interval 2. However in interval 2 the seabed contact occasionally switches polarity, which suggest small magnitudes and we get pretty high amplitudes from deeper down the sedimentary sequence with chaotic reflections.

P12 L17 - The sentence "Consequently..." makes it sound like you did this deliberately, whereas I don't think you did at all! I'd rephrase this as "Consequently, along-profile II samples the west flank of the channel rather than its crest, and therefore complicates the recorded seismic response."

P12 L17: Correct this happened unintentionally but we'll take the figure out, thanks.

P12 L17-19 - It took me quite some time to recognise what was going on with the appearance of the 'double bed' in Profile II and Figure 3. I think you need to explain the geometry more clearly, and explain that you have these two laterally-offset reflectors within a Fresnel zone of each other. I also think it would be helped if you presented Profiles III, IV and V first - they don't have to come in numerical order. That said, I do wonder if Profile II adds much to the interpretation - you don't really refer to it later in the manuscript, and it's clearly not acquired in the most ideal location (not that I blame you, of course, it happens!!). Maybe it should be relegated to supporting material?

P12 L17-19: We prefer to take it out. The figure is easily misunderstood

P12 L20-21 - Why would depth conversion obscure the sea bed?

P12 L20-21: The double ice-sea contacts and seabed reflections are caused by different pathways and thus different reflection areas of the seabed. Correct depth converting is actually impossible, what horizon do you pick for depth conversion? Either choice of ice-seawater contact (channel crest or base) will only partly convert the reflections to the correct depth.

Figure 4 - these seismic images are lovely :)

Figure 4: Thank you, detonating cord at firn works very well.

P15 L17-18 - with the likely complex pattern of reflectivity close to the uncoupling, I'm not sure you can say that the polarity 'confirms' the presence of water - but it might certainly support or imply it.

Page 15 L15-18: Agreed

Figure 6 - it might be good to include a refresher of the location map?

Figure 6: Sorry we refer to figure 1 d for the numbering. Hope that is acceptable.

Section 4.3 - again, I'm not sure that 'drainage' is yet appropriate in this section header.

Section 4.3: Agreed

P18 L11-12 - Given that the landform likely represents a diffracting point rather than a specular reflection, I'm not sure that reflectivity calculations hold. I agree with your geometric arguments and think that you do a good set of analyses here, and I think that the reflectivity argument is in any case superfluous. I'm not sure what the reflection coefficient equation would be for this; I think you can likely speculate that the amplitude appears weaker than surrounding reflections, but the quantitative assessment might be an over-interpretation. (this comes back on P19 L17-18).

P18 L11-12: I will add the raw shots, showing the feature. The feature is visible over 1200 m. That is a long distance for a diffraction. Especially SP 15, where we see a reflection splitting off the subglacial feature, shows they are probably reflections. If they had been diffractions I would expect to see them cross each other. Please let me have your judgement again with this extra image. Thanks

P20 L4 - define 'trend'. Do you mean the magnitude? As in, you're interpreting based on indicative reflectivities rather than a fully-quantitative asessment?

P20 L4: Indeed, we mean magnitude and will add this.

P20 L16 - I wonder if the terms 'disturbed' and 'undisturbed' imply a process rather than a geometry? As in, the implication that the sediment has been disturbed by something (e.g., ocean currents). Of course, this might be the case, but as an indicator of simple geometries then I think that 'stratified' and 'unstratified' of 'homogeneous' might be less weighted?

P20 L16: Indeed the term disturbed is not well chosen, we'd like to use chaotic so we refer to a "sedimentary sequence with chaotic reflections". In our answer to reviewer #2 we answer this more elaborately.

P22 L5-6 - I think flat and horizontal might be the same thing? The difference here might be in the terms 'planar' and horizontal.

P22 L5-6: We'll use flat. Thanks

P22 L19 - I agree with you, Bradley Morrell is great! Technical issues:

P22 L19: Yes now actually Daniel (Steinhage) worked with Bradley and I was shown around by Dave Routledge. We met each other at the shelf of Support Force Glacier and then did this survey together. It worked like clockwork.

There are many grammatical issues which I have flagged up in the attached manuscript. These are flagged up, and suggestions made for alternative wording; all of the comments above are also included.

Please also note the supplement to this comment: https://tc.copernicus.org/preprints/tc-2020-54/tc-2020-54-RC1-supplement.pdf

Supplement: Thank you, this is highly appreciated.

RC2:

Neil Ross (Referee)

neil.ross@ncl.ac.uk
Received and published: 3 July 2020

This is a well reported high-resolution seismic reflection survey targeting the form and physical properties of an ice shelf channel and the sub-seafloor sediments beneath it at Support Force Glacier (SFG), East Antarctica. The seismic analysis is supported by some airborne ice-penetrating radar data. The methods are sound and detailed, the description and presentation of the data is reasonably good, and the science is high-quality and of potential interest to the readership of TC. The data are hard won field geophysical data from a remote part of the Filchner Ice Shelf, Antarctica and certainly deserve to be published in some form. I do, however, have some serious concerns about the way the data are 'pitched' and argued in the current version of the manuscript. Specifically, I am very unconvinced by the association between the ice shelf channel, the "subglacial landform", and the sub-seafloor sedimentary structures, and the argument for sediment transport subsequently developed.

General comments 1. The manuscript does not engage at all with glacial-geological literature relevant to glaciomarine processes and sediment deposition in a grounding zone and ice shelf environments. Such process literature is key to understanding the sedimentary structures imaged in the seismic data. Without reference to such literature you cannot make the link between the present-day ice shelf channel and the sediments beneath the sea floor. Though there are clearly more modern literature available, a good place to start would be David Drewry's textbook on

Glacial Geological Processes (1986). What are the processes that the seismic observations of the cavity and the subsea sediments give insight into? What might be the glaciological processes that determine sedimentation in ice shelf cavities and at grounding lines?

General comments 1:

Thank you for making this point. We overlooked this and will back this up with literature and a more focused interpretation. We'd like to stress that we make an interpretation of the radar and seismic profiles so at best evidence is circumstantial. However, we do believe the interpretation we provide is the best explanation of what we observe in the seismic and radar profiles. This is also supported by the evaluation of Adam Booth, reviewer #1, one of the seismic experts in glaciology.

In our answer we'll use the following terminology:

Grounded ice:

- *Subglacial channel: a feature between the ice and the bed, probably water filled. Needs ice to be visible.*
- *Landform: a geomorphological feature of the bed, would be visible without the ice*

Ice shelf:

- *Surface channel: Meandering narrow long channel at the surface of an ice shelf*
- *Basal channel: The sub-ice shelf channel causing the surface channel through hydrostatic adjustment.*

The seismic survey concentrates at a surface channel caused by a basal channel at the ice shelf of Support Force Glacier. The basal channel is formed upstream by a subglacial channel we see in radar profiles. At the grounded ice we can track the subglacial channel at radar profiles 3, 4 and 5. At profile 3, 7.1 km upstream from the grounding line, the subglacial channel is hardly distinguishable from the bed after which its height increases at profile 4, 4.4 km upstream from the grounding line, to approximately 100 m above the surrounding bed. At profile 5,1.8 km upstream from the grounding line, the top of the channel increased to approximately 250 m above the surrounding bed.

Profile 6 lies at the grounding line: the western part has passed the grounding line, the eastern part has not. The basal channel, an extension at the ice shelf of the subglacial channel, now reached a height of approximately 300 m above the surrounding base of the ice shelf.

This is where we'd like to adjust our interpretation: Considering the comment of reviewer #1 that the refection coefficient of the off-nadir reflections is tricky (we don't think they are diffractions) and we might over interpret the data, we will only use its polarity which indicates the presence of water. The radar profiles show the subglacial channel increases its height from approximately 0 m to 300 m over a length of 7.1 km approaching the grounding line. This would place a landform within 7.1 km upstream of the grounding line which we think is unlikely. Summarizing, if we leave out the value of

the reflection coefficient we see no evidence the off-nadir reflections in seismic profile I between radar profiles 5 and 6, are caused by a landform.

We interpret these reflections to come from the subglacial channel we see in the radar profiles 3, 4, 5 and 6. The increase in size, when approaching the grounding line, is likely caused by the ocean is interacting with the subglacial channel due to tidal motion thereby increasing its size due to melting of the channel walls as suggested by Drews et al. (2017), Horgan et al. (2013) and modelled by Walker et al. (2013). The radar profiles 3, 4, 5 and 6 show the subglacial channel interacting with the warm ocean. Once passed the grounding line this wide opening of the subglacial channel adjusts to hydrostatic equilibrium and forms the basal and surface channel in which the subglacial drainage water incises.

We plan to adjust our interpretation accordingly: At the grounded ice of Support Force Glacier radar profiles 3, 4, 5 and 6 show a subglacial channel connecting a basal at the grounding line. Approaching the grounding line the subglacial channel increases its size to 300 m height at the grounding line, which we attribute to ocean interaction. This setting is similar to the subglacial estuary described by Horgan et al. (2013). Because the subglacial channel connects to the only basal channel at the western side of the ice shelf, and because we have a large subglacial drainage influx modeled at the western side of the ice shelf, we interpret the subglacial channel to be a subglacial drainage channel.

The grounded part of profile I consists of a sediment layer judging by its reflectivity becoming more consolidated closer to the grounding line. So the drainage channel probably travels over a layer of subglacial sediments with varying consolidation. The exact nature of the subglacial drainage system we do not know but the radar and seismic profiles do suggest channelized flow close to the grounding line. Possibly we are dealing with a channel that, upstream and outside the survey area, is coupled to a surrounding distributed system as described by Hewitt (2011). Close to the grounding line channelized flow is favorable which corresponds to our observations.

2. I am not, at present, convinced that the observations of the stratified sediment beneath the ice shelf channel have any bearing on the ice shelf channel and modern- day "sediment transport" itself. The manuscript makes no convincing case that the sediments were deposited by present-day processes. These sediments could be much older than the ice shelf channel and may have absolutely no relationship with modern- day processes at the grounding line or beneath the ice shelf. The authors need to either (1) provide a much stronger justification for the direct link between the sediment and the modern-day glaciology (e.g. by using the literature on glaciomarine sedimentary processes I refer to above and/or better describing and presenting the data they report). It is not enough to simply say on page 21 that "we conclude the landform is hosting the transport of sediments that are deposited in the ocean cavity close to the GL" – what is the evidence?; or (2) reframe the paper so that it is a detailed characterisation of the form and physical properties of (a) the ice shelf channel; (b) the sub-shelf bathymetry; and (c) the sub-bottom sediments of SFG, but doesn't link them directly. For what it is worth I think a manuscript describing '2' would be useful and worthwhile. We know so little about Support Force Glacier at present.

General comments 2:

To summarize our findings:

We have a modelled large influx of freshwater on the western side of the shelf.

From the airborne radar data of the shelf we know the ice shelf has only one basal channel at the western side. That must be the place where the subglacial drainage channel enters the ocean.

There is a noble gas sample downstream of Support Force Glacier suggesting a freshwater influx of terrestrial origin coming from Support Force Glacier.

Why do we think the water of the subglacial channel carries sediments?

Along profile I (along-flow, 1.5 km east of the basal channel) shows an approximately 200 m thick sedimentary sequence close to the grounding line of different character then the seabed further downstream part of the ocean cavity. The sedimentary sequence is less consolidated and has chaotic reflections and little signal loss with increasing depth. Across profile III, crossing this sedimentary sequence with chaotic reflections, shows this sequence is only present under the sub-shelf channel. Both on the far east and west side of profile III there is hardly any structure in the seabed except right under the channel. This sedimentation most likely has been transported by the subglacial channel.

Based on profile I and III we interpret the sedimentation to be point sourced and fan shaped, possibly a grounding line fan (Powell, 1990) or an ice-proximal fan (Batchelor and Dowdeswell, 2015). This explains the chaotic reflections (we referred to as disturbed), with high amplitudes in this sedimentary sequence and this material being softer as the further downstream part of the sea bed.

We realize there are concerns here as the fan has formed under an ice shelf of Support Force Glacier without surface melt, a characteristic of fans (Powell and Alley, 1997). But we do have evidence for channelized flow at the grounding line, a noble gas sample suggesting freshwater observation influx of terrestrial origin likely (Huhn et al. 2018) and a significant (190×10^6 m^3 a^{-1}) modelled channelized freshwater influx at one place on the west side confirmed by the presence of a single basal channel on the western side. We also have an unusual ocean cavity with a steeply descending seabed and, as argued in our paper, a stable grounding line. These are typical conditions for the formation of a fan at the grounding line (Powell 1990, Powell and Alley 1997, Batchelor and Dowdeswell 2015) . We will emphasize this in the text and update figure 4 with a schematic lay out as in figure 2 where we identify the sedimentary sequence with chaotic reflections.

Can we proof all this and can we say how old this sedimentation process is? Not without sea bed samples of the sedimentary with chaotic reflections or an additional seismic across-flow profile passing the subglacial channel. Do we think this interpretation is likely and sound? Yes we do if we look at the glaciological setting; a grounding line environment where a subglacial drainage channel enters the ocean cavity with a descending seabed and seismic profiles show a sedimentary with chaotic reflections right under the basal channel.

3. The assertion in the abstract and section 4.5 that the "landform is hosting the transport of sediments that are deposited in the ocean cavity close to the GL" (page 21) is very poorly supported by any evidence apart from the spatial coincidence between the landform (described in other parts of the manuscript, e.g. section 4.3, as a "subglacial drainage feature") and the ice shelf channel. What is the process that is being inferred here? In the conclusions it is suggested that the sediment

transport is by subglacial meltwater, but that is not developed from a detailed, carefully constructed and coherent argument in the manuscript.

General comments 3:

In our reaction to general comments 1 we explain our adjusted interpretation: the off-nadir reflections are probably caused by the enlarged opening of the subglacial channel, not the landform. In our reaction to general comments 2 we explain why, based on seismic profile I and III we interpret the sedimentary sequence with chaotic reflections to enter the ocean cavity through the subglacial channel.

Please don't get me wrong, I think the manuscript is full of great data and interesting observations, but at present it seems to lack a clear focus, and many of the assertations are not fully thought through or developed from a process-oriented perspective. It's all very well to justify the landform identified in the ice-penetrating radar as being comprised of sediment from the seismic reflection coefficient analysis (though it is clear that the seismic data are not perfectly acquired to do this), but the manuscript makes some very large leaps from 'this is a subglacial sedimentary landform (with possibly a bedrock core)' to the stratified sediment offshore is the direct result of focused melting from the ice shelf channel. What is the process by which this happens? It needs to be justified.

We agree we should make a better case here. We've set out our reasons as to why we think we can connect the sedimentary sequence with chaotic reflections we see in seismic profile I and III to the subglacial channelized flow and why we think this sequence probably resembles a fan.

An idealised conceptual model of the ice shelf cavity/grounding line/ice shelf channel processes and environments might be useful. See examples in Le Brocq 2013; Drews et al. 2017; and Jeofry et al. 2018 (Suppl Info). A conceptual model like these would really help pull together how the SFG system works and make the manuscript far more accessible to prospective readers. I suspect that developing one might also help the authors think through the processes and allow them to piece together a much more coherent argument and explanation for their observations.

Conceptual model: Is this like a picture explaining the model? It should be possible but it is quite some work, There are figures showing the formation of fans at grounding line like in Powell (1990). The difference in our case is that there will be a shelf at the grounding line instead of a cliff. But if you feel the paper needs it, we can provide it.

Please note that there are a few typos and minor grammatical errors throughout the manuscript that will need correcting before publication. I have highlighted some below, but I have not been comprehensive in this.

Specific comments

Page 1

Title: Support Force Glacier is East Antarctica, not West.

Title: Not changed as we stick to the definition that the EAIS lies between 45° west and 168° longitudinally.

Title: Where is the evidence for "sediment transport" in the paper?

Title is changed according to our adjusted interpretation.

Addresses: 'Natural Environment Research Council' (i.e. not National Environmental).

Addresses: Updated

Abstract (L1): "surface channels" not "flow stripes". Flow stripes are something different, and are not associated with basal ice shelf channels.

Abstract L1: Agreed, the surface channel at Support Force Glacier starts as a meandering surface channel at the grounding line, is not a flow stripe.

L5: "beneath" rather than "on"? L6: "part" of what?

L5: Corrected. Floating part should be ice shelf
L8: "initiates" rather than "forms"?

L8: Agreed

L10: What is the justification for the 200 m thick sequence of sediments being "grounding line deposits" – what is the evidence and argument for this? At present the manuscript doesn't provide this.

L10:This is an interpretation we give in our reply to the general comments. We will adjust the discussion text accordingly and will explain why we interpret this sequence as a grounding line fan.

L10: "the landform hosts the subglacial transport of sediments" – why not just "the landform is composed of sediments". That seems to be as far as you can take the interpretation of the seismic data as far as I can make out from the manuscript. There is no evidence for subglacial transport of sediments from the data presented.

L10: This will be removed as we interpret this feature no longer as a landform.

L15: "shear margins" are introduced here, but figures 1a&1b suggest that the sub- glacial hydrological pathway does not correspond to the shear margin.

L15: Indeed the channel is 4 km east of the shear margin. We will remove this.

L4: surface expressions of basal ice shelf channels are not the same as flow stripes, and sometimes they 'jump' across flow stripes. They are surface features associated with linear depressions in the ice shelf surface.

Page 2

L4: We'll remove the association with flow stripes: "They are often detected with satellite imagery like MODIS…"

L25-27: some misrepresentation of Jeofry et al. 2018 here – the hard rock landforms at Foundation Ice Stream (FIS) actually determine subglacial hydrological pathways & it is the basal water that forms the ice shelf channels, not the bedrock bumps per se. The marine landforms presented in Jeofry et al. 2018 did not "confirm" anything. That particular figure was simply included to demonstrate how common such hard bed landforms were offshore and presenting them as a plausible analogues for the ridges beneath the FIS grounded ice.

L25-27: We disagree. Jeofry et al.2018 suggest a combination of a landform incising the base of the ice which when becoming afloat will cause a surface channel and basal channel. Quote: ''we propose that the bedforms are dictating the position and form of the U channels.'' Which is also why they checked the dimensions of landforms that are indeed at completely different locations which we also state in L26, 27. As the landform also organizes the drainage pathway, quote:''the water incises upward into the corrugation peak'' also because fresh water will want to move upward will assemble in the by bedrock formed corrugation peak.

L29: I do not understand "become spots at the ice shelf base when adjusting the hydrostatic equilibrium"

L29: The surface trough of the shear margin (that has a surface depression) induces a basal channel due to hydrostatic adjustment once it passes the grounding line. Once afloat, the surface trough is shallower while adjusting but then deepens again as a warm water plume thins the base of the ice in the channel.

L32-33: I do not think that this manuscript provides information on the "type of material and structure of the bed upstream of a basal channel". Yes the apparently offline seismic reflection in figures 2&8 is analysed to suggest that it is composed of unconsolidated sediments, but it certainly doesn't reveal the structure of the subglacial bed.

L32-33: Indeed, we state that this observation is often missing, nothing more.

Page 3

L4: it is interesting to note that the modelled subglacial outflow in figure 1b does not map exactly against the ice shelf channel (i.e. they are offset by ~5 km despite a new high-resolution bed topography of the SFG trunk).

Page 3

L4: This is correct, the modeled drainage pathway is offset by 4 km from the basal channel. This model is coarse, it has a resolution of 1 km and does not take the physical nature of the bed into account that may steer the pathway somewhat differently. Although we did use the topography derived from the airborne radar data, the surrounding is of course still BEDMAP2. So the model is an indication of where one may expect a subglacial drainage system.

L8: "into the precise"

L8:Agreed

L9: "typically penetrate"? There are some examples.

L9: Agreed.

L11: I do not understand "..or does the substrate also consist of sediments in which case we can expect recent sedimentation on the seabed?" – even if the bed is hard bedrock you can still have sedimentation on the seabed by (a) subglacial erosion of bedrock; and (b) transport of sediment from upper parts of a glaciers catchment underlain by sediment.

L11: Thanks for making this point, we will rephrase ''or does the substrate also consist of sediments."

L16: "supported" rather than "backed up"?

L16: Agreed

L17: "continue" rather than "proceed"

L17: Agreed

L18: "active/current" subglacial drainage?

L18: Agreed

L23-24: Support Force actually lies between Academy Glacier and Recovery Glacier. It may also be worth making clear that "northwest" is "grid northwest".

L23-24: Thanks, corrected

L24: "constrained" rather than "tugged in"?

L24: Agreed

L30: reference Bedmachine as well/instead of Bedmap2?

L30: Just BEDMAP 2.

L33: I would not describe the survey as a "grid". Refer to figure 1 at the end of line 33.

L30: Agreed

Page 4

L2: "Ice surface velocities"?

Page 4

L2 : Correct, thanks

L11: I do not believe that the DLR acronym has been defined earlier in the manuscript.

L11: We will correct this

L14: Jeofry et al. ESSD, 2018 might be a better reference than Rippin et al.? see https://essd.copernicus.org/articles/10/711/2018/

L14 Jeofry et al: Good suggestion, thanks

L14: think you mean 312.5 Hz here? See section 2 of https://agupubs.onlinelibrary.wiley.com/doi/full/10.1029/2018GL077504

L14: Correct

L16: "laser surface terrain"?

L16: Correct

L27: Paden et al. reference is 2010 in reference list? Please also be specific about which years of OIB data were used (e.g. up to Dec 2018 Antarctic surveys)?

L27: Thanks for bringing it to our attention. The reference should be:
Paden, J., Li, J., Leuschen, C., Rodriguez-Morales, F., and Hale., R.: 2010, updated 2018. IceBridge MCoRDS L2 Ice Thickness, Version 1. Antarctica., Boulder, Colorado USA. NASA National Snow and Ice Data Center Distributed Active Archive Center.,https://doi.org/10.5067/GDQ0CUCVTE2Q, 2019.

L30: how extensive was the model domain for the hydrological routing presented in 1b? Was it just the domain shown in 1b, or was it more extensive (e.g. entire SFG catchment)?

L30: The model domain for the routing was the entire hydrological catchment of SFG. I attached a small figure, which we could put into the answer or appendix.

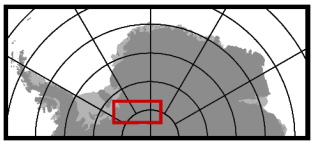

Page 5

Figure 1: Please annotate start and end of seismic lines in figure 1 and corresponding seismic profile figure.

Page 5

Figure 1:We provided arrows at each line (Fig 1b).

L1: as stated previously, the modelled subglacial meltwater outflux location does not correspond that well with the surface channel, despite the new high resolution ice thick- ness/bed data.

L1: As explained (Page 3, L4) we use a model with its shortcomings. The main result is we can expect water drainage on the western side of the shelf. Keeping in mind that the resolution of the model is 1 km, and does not take the physical properties of the bed into account, we find 4 km acceptable.

Page 6

Table 1: Why is it important to have the column "position from GL"? From which part of the profile is this measured? Suggest deleting it.

Page 6

Table1: We will remove this

Pages 7-9

Given the expertise of reviewer 1 I have not assessed the description of the seismic methods in detail.

Page 10

L16: After "ice shelf thickness." it might be a good idea to refer to figure 1 to provide an example of the artefacts.

Page 10

L16: Reviewer #1 pointed out that the phrase artefact is not accurate. We'd like to change the title to "seabed depth conversion" as he suggests.

L18: “structure of the seafloor” or “morphology of the seafloor”?

L18: The morphology is a better phrase

L20: Figure 2 should be split into 2a and 2b, rather than TOP and BOTTOM. Therefore, sentence should begin “Figure 2a shows. . ..”

L20 Figure 2: Agreed

L20 (and throughout manuscript): Delete references to along-profile and across-profile, just label the profiles I-V (e.g. “profile I” rather than “along-profile I”). L21: Start “Figure 2b. . .”

L20: Agreed

L24 (and throughout manuscript): “reflectivity zones” rather than “intervals”. These zone should also be clearly marked on figure 2.

L24: They are marked with double headed arrows on top of the figure: interval 1, 2, 3 and 4.

L28: call figure 1 after “interferometry”

L28: Agreed

L30: “uncoupled” – uncoupled from what? Do you mean “floating”? Page 11

L30: Yes we mean floating

Figure 2: label ‘a’ and ‘b’. Need to annotate the start and end of the seismic line (see comments on figure 1).

Page 11

Figure 2: labeling agreed. The shot numbering gives the shooting directions, but we can add this if you feel this is not clear.

Note that where “bed” is annotated in 2a it is not actually the ‘bed’. It is the subsea sediments.

Note: Is seabed acceptable? If we talk about sediments we are interpreting.

What is the weak reflection between ~SP46 and ~SP160 (between the labels “ICE” and “BED”)?

Weak reflections: The are probably side reflections of the ice-sea contact, the polarity is reversed just as the identified seabed contact which is why we think they resemble ice-seawater contacts. The shelf base here has a lot of topography

Please define the different reflectivity zones in figure 2 (see comments above). Provide zoomed-in views of all the detailed features described in section 3.2.

Reflectivity zones: As mentioned we have defined the intervals and they are based on structure on the bed, ice-sea contact and/or seabed. We find reflectivity does not cover the separation of the intervals properly. Please let me know if you find this ok. We can provide zooms of key features.

L1: ". . ..elongated feature above the flat bed. . .."?

L1: Based on shot spacing and two-way travel time the dimensions are 1200 m long and the feature appears to be 50 m higher than the surrounding bed if it was nadir, hence we called it elongated although of course we do not know the across-flow dimension.

L3-4: I suggest that this reflection not be described as a "subglacial drainage feature" at this point in the manuscript. Later in the paper, the reflection is interpreted as a "landform" anyway, so it is very confusing. Simply describe it a reflection at this stage, and then only once section 4.3. has been worked through should it be described as a "landform". It would be useful to have the zoom in of the reflection in figure 2 rather than figure 8.

L3-4: We propose to call this "subglacial feature". We will provide a zoom of this subglacial feature in our response to reviewer#1 as we think we are dealing with reflections. As mentioned this part of our interpretation we want to change: We interpret this subglacial feature still as off-nadir reflections but no longer as a landform but as the top of the subglacial channel that in this area so close to the grounding line likely interacts with the ocean. This interaction with the ocean probably caused a rapid increase in height of the subglacial channel.

As reviewer #1 pointed out, a quantitative analysis its reflectivity is tricky as we have a complex subglacial structure off-nadir. To avoid over-interpretation we will not use the calculated reflection coefficient but its polarity.

L6 (and throughout manuscript): "anticlines" – this is a specific geological term not normally used in the description of morphology. I recommend "concave cavity" instead.

L6: Agreed, concave cavity is a better term.

L8: "ocean cavity thickens" (rather than deepens)?

L8: Agreed

L10: what is the observation that constrains the sediment thickness to 200 m? I don't see a clear sediment-bedrock reflection at 200 m in Figure 2, so do the authors instead mean "of at least 200 m"?

L10 200m: It is as you observe, there is not a clear last sediment-bedrock reflection but the chaotic reflections fade out with increasing depth. Hence approximately 200 m.

L10 (and throughout manuscript): what is meant by "transparent"? How can a material be transparent yet stratified and disturbed?

L10 transparent: What we mean by transparent is that the seismic signal penetrates deep in the formation with little loss of amplitude.

We will use the phrase (sedimentary) sequence with chaotic reflections and little signal loss with increasing depth or shortened: sequence with chaotic reflections.

as mentioned in our reaction to general comments 2.

Page 12

L15: Call figure 1 after "at the same distance"?

Page 12

L15 Agreed

L20: call figure 3 after "have been marked"?

L20: As this a complicated profile with two ice-sea contacts and two sea-seabed contacts, we'd like to take this figure out of the paper as reviewer 1 suggests. We hardly use it in our interpretation and the figure is complicated to explain.

L21: After "the seabed" add "so is not presented here"?

L21: Yes the seabed is present here as we have the seafloor returns twice (two different ray paths: path 1 is along crest of the channel, path 2 is along base of the ice next to the channel and they likely have the same seabed depth. Converting the time migrated section to depth is not really possible as we must choose one of these two ray paths to convert to depth but then we automatically misplace the reflections of the other ray path.

L22: "sequence of stratified sediment" rather than "stratification sequence"? If the authors are trying to avoid interpretation here, then it shouldn't even be "stratification sequence", it should be a geophysical description like "a series of horizontal reflections".

L22: We will remove Figure 3 as profile II is difficult to interpret and probably causes misunderstandings. As reviewer #1 pointed out, profile II hardly contributes to the interpretation.

L23: “of stratification below the basal channel” rather than “.. of a stratification sequence in the basal channel”. The seabed and sub-bottom sediments are not in the basal channel.

L23: Will be removed

L24: call figure 3a at end of sentence.

L24: Will be removed

L31: “terraced” not “terrace-shaped”

L31: Thanks

L32 (and throughout manuscript): instead of “as indicated in Figure 4” just have “(Figure 4)”. There are a lot of wasted words throughout the manuscript when fig- ures are being called. Authors should make their statement/describe the data etc. and then simply cite the relevant figure at the end of the sentence. See Box 1 of https://aslopubs.onlinelibrary.wiley.com/doi/full/10.1002/lol2.10165 for a better explanation of what I mean. There is also no need to repeat figure caption information in the text (e.g. page 12, line 26 opening line of section 3.4).

L32: Thanks for pointing this out

Page 13

Figure 3: what are the reflections above the seabed? It is not clear in the figure what all the complex reflections are. More annotation is required.

Page 13

Figure 3: There are two seabed reflections present due to different travel paths. See our reply at L21. Anyway we will remove Figure 3

Figure 3: Again, authors should not refer to sub ice shelf sediments as “bed”. Bed should only be used when referring to grounded ice.

Figure 3 bed: We used the term seabed which we do find in literature.

L3-7: This paragraph should refer to figure 4.

L3-7 Agreed

L6-7: I do not think that I understand the sentence “The across-profiles. . .. . ..across- profile III”. I have a suspicion, however, that this sentence might actually be quite key to the authors’ suggestion that there is a relationship between the ice shelf channels and the sediment beneath it. If I understand it correctly, here they are suggesting that there is a thicker stratified sequence in the

parts of the sub-sea sediments directly beneath the ice shelf channel. Is that correct? At the very least, the authors need to annotate the thicker sequence below the ice shelf channels to assist the reader understand exactly what is being described here.

L6-7: Yes that is what we claim, right under the basal channel, profile III shows thicker stratification (roughly from SP 3 to SP 24) under the basal channel then outside the basal channel. We plan to add schematic images (recommendation of reviewer 1) of profiles 3,4 and 5 as in Figure 2 marking the stratification areas.

Page 14

Figure 4: This figure appears to be critical to the argument that the sediments beneath the ice shelf channel were deposited by the ice shelf channel (i.e. there is a spatial coincidence between the channel and a thick sequence of sediments subsea). What is the thickness of the sediment package beneath the ice shelf channel in figure 4a (note that figure subplots need to be labelled throughout the manuscript)? Is it, as implied by the y-axis, 400 m? If so, that is a phenomenal amount of sediment to be deposited 40 km from the grounding line solely from melting beneath an ice shelf channel. The authors should calculate the sedimentation rate for this package of sediment. Is it possible for their sedimentation rate to be valid (e.g. assuming a certain proportion of sediment in the ice, and known melt rates for ice shelf channels as calculated from ApRES). Figure 4 needs to be better described in the text and the key features (e.g. sediment packages) need to be better annotated. I assume that the ages of transit time from grounding line are based on current ice velocity (i.e. figure 1a)?

Page 14

Figure 4: Indeed I see the confusion. Profile V (as profile IV) has multiples causing apparent stratification. This is clearer to spot in the time migrated profiles. So no, there is not 400 m of stratification at profile V (Figure 4a), I come to no more than 100m. We will provide a schematic picture with our interpretation. The focus of the paper lies on the sedimentary sequence with chaotic reflections that profile III crosses.

Page 15

Figure 5: why not just make this a 3D figure and show all 4 profiles (figure 2b of https://agupubs.onlinelibrary.wiley.com/doi/full/10.1029/2010GL042884 is an example of what I mean)?

Page 15

Figure 5: Thanks for the suggestion. What we like to provide is use both radar and seismic profile to show the development of the subglacial channel (grounded) and how this continues as a basal channel under the ice shelf.

The present figure actually consists of 3 profiles, profile 4 is used twice. Reason why we displayed them like this is to get a good handle on where melt/widening of the basal channel takes place.

L5-12: There is lots of text in this paragraph that is direct repetition of the figure caption of figure 6.

L5-12:We will clean this up

L5: "We selected ten across ice radar profiles. . .."?

L5: Agreed

L6: what is the evidence for the subglacial landform "shaping the channel upstream of the GL"? How does it do this, and what is the process?

L6: We withdraw this interpretation

L11-12: This sentence needs some expansion to make 100% clear the spatial coincidence between the landform and the ice shelf channel. Reference to figure 1 would help too. I don't understand the phrase ". . . after which the landform become indistinguishable from the bed"? Surely if it is a basal landform it is the bed? It would also be useful to get a better idea and description of the wider bed topography around the landform (e.g. entire bed of SFG) to understand the context. Figure 1b is of little use in this regard its colour scheme is very uninformative.

L11-12: We will adjust our interpretation as we state in our reaction to general comments 1 and remove the concept landform. Looking at the radar profiles 3, 4, 5 and 6 we see that the subglacial channel we see at the grounded ice, increases in size as it approaches the grounding line. So there is no landform at the grounded ice, just a subglacial channel that increases its size due to interaction with the ocean.

Line 15: again, lots of text that should be in the figure caption, or already is. Page 16

L 15: Agreed

Figure 6: Indicate very clearly which radargrams are over grounded ice and which ones are over floating ice.

Figure 6: Agreed that should be made clearer. Profile 6 lies at the grounding line.

Figure 6: are the authors absolutely sure that radar profile 5 is fully grounded all the time? Could there be tidally-induced grounding line migration?

Page 17

Page 17

Figure 6 profile 5: We have no indication profile 5 is susceptible to grounding line migration. Profile 5 crosses seismic profile I at SP 5 where we have a positive basal reflection indicating

consolidated material. To us that means the ice is grounded here. If ocean water would have reached this far it would have influenced the reflectivity.

We do have an indication the MOA grounding line, crossing seismic profile I at SP 51, is not correct. Seismic profile I clearly shows ocean water being present upstream of the MOA grounding line down to SP 26.

Are we sure profile 5 is fully grounded all the time? No but it is very likely.

Section 4.1: It is a little difficult to link section 4.1 with figure 1, as the text in section 4.1 refers constantly to shot points, but these are not apparent on figure 1.

Section 4.1: We will be clearer here. We wish to refer to figure 2, profile I here, and will add this in the text. The interferometric grounding line crosses profile I at SP 23 but this can't be chosen that precise, . The polarity switch at profile I lies at SP 26, so 150 m downstream of SP 23. This deviation may be caused by the unprecise choice of the grounding line here.

Line 14: "topographically constrained flow"?

L14: Correct

Page 18

Figure 7: it took me quite a while to figure out exactly what this figure was. I suggest that it simplified by removing the bed profile picks. The key point of this figure is to conceptualise the idea of the offline reflection. Is the red semi-circle a "possible drainage feature" or it is a "landform"?

Page 18

Figure 7: We think the concept of Figure 7 is still not clear.

The figure should show that off-nadir reflections of the landform (represented by the radar profiles 5 and 6 and we now interpret as the subglacial channel) arrive at the same time as if there had been a 50 m high channel at nadir (represented by the red semi-circle). As reviewer #1 points out, the weakness of the reflections shown in figure 8 (a zoom of profile I, figure 2) already suggest these reflections (or diffractions as reviewer 1 points out) are off-nadir.

Section 4.3: I recommend not describing the feature being evaluated as either a "subglacial drainage feature" or a "landform" until the authors actually determine which of the two hypotheses are their preferred one. Whilst the unusual (offline?) reflection they describe is referred to throughout as a "subglacial drainage feature" the author then state on page 19 lines 16-17 that they "prefer interpretation 1" which is that the reflection is from the landform. This is a bit of a mess, and suggests that the authors have changed their preference during the writing of the manuscript but not updated all parts of the manuscript. A "landform" is not a "subglacial drainage feature".

Section 4.3: Indeed, we adjusted our interpretation as described in our reaction to general comments 1 and will adjust the text accordingly.

Section 4.3: change heading to "Does the seismic data record a subglacial drainage feature or a subglacial landform?" or something along those lines. Section 4.3 evaluates these two hypotheses on the basis of the seismic data and geophysical theory. The section heading should reflect that in some way.

Section 4.3: We will restructure this according to our interpretation: The reflections are off-nadir and represent the subglacial channel. The channel opening is enlarged here due to interaction with the ocean. This interaction between ocean and a subglacial channel is described by Horgan et al. (2013)

Line 13: provide some additional detail about what is meant by a "separate drainage feature on a hard bed" – In essence this is a Röthlisberger (R-) channel incised into the overlying ice and should be described as such here.

L13: Indeed if the reflections are at nadir it would seem like an R-channel and that is represented by the red semi-circle. That this is most likely not the case is because there is only one basal channel visible at the western side of the ice shelf and we argue that this is where the subglacial channel enters the ocean cavity which is on the western side so off-nadir of profile I. Had the reflections been nadir, the R-channel would have entered the ice shelf elsewhere but we see no evidence of another basal channel in the radar data. That is our main argument as to why we think the reflections are off-nadir and are caused by the subglacial channel.

Page 19

L17-20: This is an important admission here, and one that is entirely inconsistent with the title of the manuscript "Subglacial sediment transport upstream of a basal channel. . ...". So far, the data don't even unequivocally demonstrate the presence of subglacial sediments.

Page 19

L17-20: Correct, it is an interpretation.

Page 20

L14: "floating ice" rather than "uncoupled ice"?

Page 20

L14: Correct

L16 (and throughout manuscript): what do the authors mean by "disturbed"? This needs defined and highlighted/annotated in a figure. Do the authors mean "deformed" sediments or stratigraphy?

L16: We propose chaotic reflections and little signal loss with increasing depth, as mentioned in our reaction to general comments 2.

L17-19: apart from the reflection coefficient values and the "disturbed and stratified" stratigraphy, what other lines of evidence for these materials being grounding line de- posits do the authors have? This is where reference to glacial geological literature is essential.

L17-19: We are presenting an interpretation. Seismic profile I and seismic profile III most likely show the presence of a grounding line fan.

L31: ". . .are positioned on the western side of SFG near its shear margin."?

L31: Agreed

L32: I disagree that you can track the landform at least 7.7 km. It is not apparent in profile 3 (Figure 6), so it can therefore be tracked for a maximum of 5.2 km (i.e. up to profile 4).

L32: If you follow the same flow line along profiles 3, 4, 5 and 6 (marked on the long profiles with an arrow and radar trace number it is quite obvious. We also have 38km long profiles that make a clearer case for this observation which we can provide possibly in a supplement.

L33: "some degree of consolidation" – so is it unconsolidated sediments, or not?

L33: As we pointed out in the our reaction to general comments 1 we will withdraw the quantitative analysis of the reflectivity. We will just use the polarity of the off-nadir reflections.

Page 21

L1-23: I am totally unconvinced at present by the argument the authors make linking the sub cavity sediment stratigraphy with the ice shelf channels. I see no evidence at all that (a) sediment is being discharged at the grounding line from a subglacial hydrological channel; or (b) that sediment is being deposited directly from basal melt within the ice shelf channel. There seems to be a huge leap of faith being made in this part of the discussion, particularly in L4-5 i.e. "Taking the evidence together we conclude the land- form is hosting the transport of sediments that are deposited in the ocean cavity close to the GL" – I see absolutely no evidence presented in this manuscript supporting the transport of sediments. If the authors wish to pursue this angle in a revised manuscript then they will also need to explain the transport mechanism. Is it subglacial deformation advecting sediment to the grounding line? Is it sediment transport by subglacial meltwater? Or, is it englacial sediment transport and then melt out?

Page 21

L1-23: There is clear evidence of subglacial drainage at the western side namely the basal channel itself which matches a modelled subglacial drainage pathway with a large water flux. The radar profiles 3, 4, 5 and 6 indicate the presence of a subglacial channel matching the location at the grounding line of the basal channel. The increase in height of the subglacial channel seen on profiles 4,

5 and 6, close to the grounding line can very well be explained by interaction with the ocean. This is what one would expect of channelized flow close the grounding line and has been suggested by Horgan et al. (2013) and Drews et al. (2017) and modelled by Walker et al. (2013) and Hewitt (2011). What we can't proof is that this channel is carrying sediments but it is likely that at the end of an ice stream the subglacial channelized drainage system carries sediments. We do have the observation in seismic profiles I and III, of a sedimentary sequence with chaotic reflections close to the grounding line (profile I) and the presence of this package only under the basal channel (profile III), exactly where one would expect sedimentation to take place if the subglacial channel would be carrying sediments.

L12-14: Here, the authors state "What we do see is more stratification in all across- profiles below the sub-shelf channel than outside of it and that this stratification extends to the eastern side of across-profile III." If this is the case then this is potentially important, but at present (except perhaps a hint on page 13) this observation is not effectively presented in the current version of the manuscript. This needs strengthened considerably if the authors are to underpin their argument robustly. I remain unconvinced though that their survey layout is extensive enough to permit this statement. I would also like to see an assessment of the implications of thinner ice (and therefore < englacial signal attenuation) over the ice shelf channels – could this lead to higher amplitudes reflections from subsea interfaces beneath the channels compared to the sediments beneath the thicker ice beyond the channels? I also think that the authors need to carefully consider the entire sediment package (i.e. the stratigraphic relationships between the sediment beneath the ice shelf channels and those beyond the channels).

L12-14: Profile III shows thick sedimentation only under the basal channel consisting of several levels and extending eastward. We agree we should emphasize this observation and it's interpretation more. This is what links the sedimentation to a grounding line fan where the subglacial channel enters the ocean cavity and forms the basal channel by adjusting to the hydrostatic equilibrium.

Profile IV and V have also show sedimentation but are tricky as multiples occur between stronger reflections. See my reaction to your comments at Figure 4. These profiles also cross different formations that are beyond the focus of the paper.

When calculating a reflection coefficient, the attenuation in ice and seawater over the entire travel path are taken into account as is pointed out in chapter 2.6, equation 2. As such reflectivity is compensated for the attenuation.

L29: My understanding of reflection coefficient analysis is that it characterises the physical properties of the upper few metres below the interface. As such it is a stretch to state "the eastern side of the landform consists of sediments. . .". Perhaps make this statement more specific (e.g. "Reflection coefficient analysis indicates that the upper few metres of the landform is unconsolidated sediment. . .")?

L29: The reflection coefficient characterizes the interface between two media but if there is a layered sequence the reflection coefficient can be influenced by interference. We will just stick to the polarity of the off-nadir reflections.

L31: OK, so here, finally in the conclusions section, the authors are specific about the actual process they believe is at play, i.e. "The landform hosts a channelized subglacial drainage which transports sediment downstream". I therefore ask the following questions (1) what is the evidence for subglacial drainage? (2) how does a landform "host" channelized subglacial drainage? (3) where is the evidence for sediment transport?

L31: Evidence for subglacial drainage I pointed out answering your comments at page 21, L1-23

The subglacial feature is most likely the subglacial channel interacting with the ocean as pointed out in the our reaction to general comments 1.

Profiles I and III are evidence of a grounding line fan under the basal channel.

L32: How do the authors know that the 200 m thick sediment package has any association with the current processes at the grounding line? These sediments could be ancient and have nothing to do with modern-day grounding line processes. The spatial relationship could merely be coincidence.

L32: As mentioned quite extensively in our reaction to general comments "we do have evidence for channelized flow at the grounding line, a noble gas sample suggesting freshwater observation influx of terrestrial origin likely (Huhn et al. 2018) and a significant (190 x 10^6 m^3 a^{-1}) modelled channelized freshwater influx at one place on the west side confirmed by the presence of a single basal channel on the western side.

Seismic profile I and III suggest the sedimentary sequence with chaotic reflections is point sourced and fan shaped, possibly it is an ice-proximal fan (Batchelor and Dowdeswell, 2015). This explains the chaotic reflections and this material being softer as the further downstream part of the sea bed.

We also have an unusual ocean cavity with a steeply descending seabed and, as argued in our paper, a stable grounding line. These are typical conditions for the formation of a fan at the grounding line (Powell 1990, Powell and Alley 1997, Batchelor and Dowdeswell 2015) ."

Lastly we do not provide hard evidence but an interpretation.

Page 22
L18: Since reviewer 1 has sung the praises of Bradley Morrell, I will sing the praises of Dave Routledge - A brilliant field guide - he's also great!

Page 22

L18: Indeed

Final comment: I appreciate that the majority of comments above will be viewed by the authors as perhaps overly negative. However, I do want to emphasise to the authors that I have provided the comments above because I feel that the acquired data are excellent and potentially very important.

I would certainly like to see these data and results being published in some way, but I do believe that a stronger more care- fully thought-through and coherent argument needs to be developed to place the assertations and findings put forward on a more secure foundation. I do hope that the comments provided above will assist the authors to achieve this.

Dr Neil Ross Newcastle University 3rd July 2020

Final comment: Your comments are highly appreciated. They force us to built up our case better which improves the manuscript. So thank you.

Coen Hofstede, August 15, 2020

References:

Batchelor, C., & Dowdeswell, J., 2015. Ice-sheet grounding-zone wedges (GZWs) on high-latitude continental margins. Marine Geology, 363 65-92. https://doi.org/10.1016/j.margeo.2015.02.001

Drews, R., Pattyn, F., Hewitt, I. et al. Actively evolving subglacial conduits and eskers initiate ice shelf channels at an Antarctic grounding line. Nat Commun ***8,*** *15228 (2017). https://doi.org/10.1038/ncomms15228*

Hewitt, I. (2011). Modelling distributed and channelized subglacial drainage: The spacing of channels. Journal of Glaciology, 57(202), 302-314. doi:10.3189/002214311796405951

Horgan, H. J., Alley, R. B., Christianson, K., Jacobel, R. W., Anandakrishnan, S., Muto, A., Beem, L. H., & Siegfried, M. R. (2013). Estuaries beneath ice sheets. Geology*,* 41*(11), 1159-1162. https://doi.org/10.1130/G34654.1*

Huhn, O., Hattermann, T., Davis, P. E. D., Dunker, E., Hellmer, H. H., Nicholls, K. W., Østerhus, S., Rhein, M., Schröder, M., and Sültenfuß, J. , 2018. Basal Melt and Freezing Rates From First Noble Gas Samples Beneath an Ice Shelf, Geophysical Research Letters, 45, 8455–8461, https://doi.org/10.1029/2018GL079706, https://agupubs.onlinelibrary.wiley.com/doi/abs/10.1029/2018GL079706.

Powell, R.D., 1990. Processes at glacial grounding-line fans and their growth to ice-contact deltas. In: Dowdeswell, J.A., Scourse, J.D. (Eds.), Glacimarine Environments: Processes and Sediments. Geological Society of London Special Publication 53, pp. 53–73

Powell, R.D., Alley, R.B., 1997. Grounding-line systems: processes, glaciological inferences and the stratigraphic record. In: Barker, P.F., Cooper, A.C. (Eds.), Geology and Seismic Stratigraphy of the Antarctic Margin II. Antarctic Research Series 71. American Geo- physical Union, Washington, DC, pp. 169–187.

Walker, R.T., Parizek, B.R., Alley, R.B., Anandakrishnan, S., Riverman, K.L., and Christianson, K., 2013, Ice-shelf tidal flexure and subglacial pressure variations: Earth and Planetary Sci-ence Letters, v. 361, p. 422–428, doi:10.1016/j .epsl.2012.11.008.

Mayor changes made in the resubmission:

Title:
Changed, the focus now lies on a grounding line fan below the basal channel of Support Force Glacier

Abstract:
Adjusted accordingly and includes our adjusted interpretation that the subglacial feature represents the top of a subglacial channel

Results:
Figure 3 showing profile II has been removed and is not discussed in the paper.
Figure 5 has been added showing a schematic diagram of the subglacial channel based on the basal ice reflection of the migrated radar and seismic profiles.

Discussion:
Changed the sequence of the items in the discussion. We discuss:

- the grounding line, the ocean cavity,
- the seismic facies of the seabed,
- a shortened discussion of the subglacial feature which we now interpret as the top of the subglacial channel connecting to the basal channel. We removed Figure 8,
- the subglacial hydrology and our arguments why the 200 m sedimentary sequence with chaotic reflections are most likely a grounding line fan

Conclusions have been changed accordingly

~~Subglacial sediment transport upstream~~ Evidence for a grounding line fan at the onset of a basal channel ~~in~~ under the ice shelf of Support Force Glacier (West Antarctica) ~~, identified~~ revealed by reflection seismics.

Coen Hofstede[1], Sebastian Beyer[1], Hugh Corr[3], Olaf Eisen[1, 2], Tore Hattermann[4], Veit Helm[1], Niklas Neckel[1], Emma C. Smith[1,*], Daniel Steinhage[1], Ole Zeising[1], and Angelika Humbert [1, 2]

[1]Alfred Wegener Institute, Helmholtz Centre for Polar and Marine Research, Am Handelshafen 12, 27570, Bremerhaven, Germany
[2]University of Bremen, Klagenfurter Straße 28359, Bremen, Germany
[3]British Antarctic Survey, National Environmental Research Council, Cambridge, CB3 0ET, UK
[4]Norwegian Polar Institute, Framsenteret, Hjalmar Johansens gate 14, 9296 Tromsø, Norway
[*]Now at: School of Earth and Environment, University of Leeds, Leeds, LS2 9JT, UK

Correspondence: Coen Hofstede (coen.hofstede@awi.de)

Abstract. ~~Flow stripes~~ Curvilinear channels on the surface of an ice shelf indicate the presence of large channels at the base. ~~Modelling~~ Modeling studies have shown that where these surface expressions intersect the ~~groundling~~ grounding line, they coincide with the likely outflow of subglacial water. An understanding of the initiation and the ice–ocean evolution of the basal channels is required to understand the present ~~behaviour~~ behavior and future dynamics of ice sheets and ice shelves. Here, we present focused active seismic and radar surveys of a basal channel~~and~~ , ~950 m wide and ~200 m high, and its upstream continuation ~~on~~ beneath Support Force Glacier which feeds into the Filchner Ice Shelf, West Antarctica. ~~We map the structure of the basal channel at the ice base in the grounded and floating part and identify the subglacial material within the grounded part of the channel and also along the seafloor. Several kilometers upstream of the grounding linewe identify a landform, consisting at least in part of sediments, that forms the channel at the ice base.Immediately seaward of the grounding line~~Immediately seaward from the grounding line, below the basal channel, the seismic profiles show ~~a~~ an 8 km long, 3.5 km wide and 200 m thick ~~partly disturbed, stratified sediment sequence at the seafloor, which~~ sediment sequence with chaotic reflections we interpret as ~~grounding line deposits. We conclude that the landform hosts the subglacial transport of sediments entering Support Force Glacier at the eastern side of the~~ a grounding line fan deposited by a subglacial drainage channel directly upstream of the basal channel. Further downstream the seabed has a different character, it consists of harder, stratified consolidated sediments, possibly bedrock, deposited under different glaciological circumstances. In contrast to the standard perception of a rapid change in ice shelf thickness just downstream of the grounding line, we find a very flat topography of the ice shelf base with an almost constant ice thickness gradient along-flow, indicating only little basal melting, but an initial widening of the basal channel, ~~which~~ we ascribe to melting along its flanks. Our findings provide a detailed view of a more complex interaction ~~of grounded landforms, ice stream shear margins~~ between the ocean and subglacial hydrology to form basal channels in ice shelves.

Copyright statement. TEXT

1 Introduction

Ice shelf channels (Drews, 2015), also known as channels (Alley et al., 2016), surface channels (Marsh et al., 2016) or M-channels ~~(?) are narrow~~ (Jeofry et al., 2018b) are narrow (a few km wide and 20–30 m deep mostly) long channels on the surfaces of ice shelves. They are often remotely detected ~~as flow stripes~~ with satellite imagery like MODIS ~~,~~ (Moderate Resolution Imaging Spectroradiometer, (Scambos et al., 2007)) or Landsat 8. These channels are a surface expression of a sub-ice shelf channel (Le Brocq et al., 2013), also known as basal channel (Marsh et al., 2016; Alley et al., 2016, 2019) or U-channel ~~(?)~~(Jeofry et al., 2018b), most often aligned to the ice flow direction but occasionally migrating across the ice flow direction. They typically are a couple of hundred metres high and a few km wide (Jeofry et al., 2018b; Drews et al., 2017). As locations of thinner ice these channels can induce ice shelf fracturing (Dow et al., 2018). Thus ice shelf channels potentially influence ice shelf stability, which in turn provides stability of the ice sheet through the buttressing effect (Thomas and MacAyeal, 1982; Fürst et al., 2016). Alley et al. (2016) categorized three types of basal channels: (1) ocean sourced channels that do not intersect with the grounding line, (2) subglacially sourced ~~channel that intersect with~~ channels that intersect the grounding line and coincide with modeled subglacial water drainage and (3) grounding line sourced types that intersect the grounding line but do not coincide with subglacial drainage of grounded ice. ~~(~~In the following we will use the term surface channel and basal channel to make a clear separation. ~~)~~

In the grounding line area of the Antarctic Ice Sheet, the location of modeled channelized meltwater flow ~~at the Antarctic ice sheet~~ often coincides with basal channels (and its surface expression, the surface channel) in the grounding line area (Le Brocq et al., 2013). This suggests subglacial drainage contributes to the formation of ~~sub-ice~~ basal channels. According to Jenkins (2011) subglacial meltwater entering the ocean cavity at the grounding line forms a plume entraining warmer ocean water and causes increased subglacial melt beneath the ice shelf which drives the further evolution of channel geometry. This hypothesis is often graphically supported by an idealized and conventional geometry of the sheet–shelf transition at the grounding line area: the ice–water contact (the underside of the ice shelf) rises steeply ~~passing~~ beyond the grounding line, thus allowing fresh water influx to form uprising melt plumes and then leveling out more horizontally further downstream (Le Brocq et al., 2013; Drews et al., 2017).

Drews et al. (2017) linked the formation of a basal channel to a potential esker upstream of the grounding line, noting that the channel dimensions are an order of magnitude larger then eskers in deglaciated areas. However, Beaud et al. (2018) found that eskers are more likely to form under land terminating glaciers. ~~?~~ Jeofry et al. (2018b) concluded that the basal channels at Foundation Ice Stream were initially formed by hard rock landforms upstream of the grounding line. Bathymetric surveys at different locations showing hard bedded landforms of similar dimensions as the basal channels confirmed this as a possibility. Alley et al. (2019), however, argued that shear margins of ice streams develop surface troughs continuing downstream of the grounding line. Once afloat, these surface troughs ~~become spots at the ice shelf base when adjusting the~~ lead to the formation of basal channels during adjustment to hydrostatic equilibrium, thereby forming a basal channel. Thus a channelized warm water

plume is likely to incise a basal channel forming observed polynyas at the ice shelf front. Both hard rock ~~bedforms~~ landforms and surface troughs at shear margins of ice streams seem to cause basal channels. Unfortunately, ~~often~~ key observations are often missing, e. g. on the type of material and structure of the bed upstream of a basal channel.

From noble gas samples at six locations beneath the Filchner Ice Shelf, Huhn et al. (2018) estimated ~~an~~ a total freshwater influx of 177 ± 95Gt/a, entering the Filchner Ice Shelf. At one location, downstream of Support Force Glacier (SFG), the noble gas sample indicated crustal origin and thus part of the freshwater influx having a grounded subglacial origin. We also know that the west side of SFG, where ~~an~~ a surface channel is present, coincides with modeled channelized subglacial drainage (Le Brocq et al., 2013; Humbert et al., 2018). Thus we have good reason to assume there is subglacial drainage channel present at SFG.

Most field observations of surface channels and basal channels come from satellite imagery, airborne or ground penetrating radar. Although airborne radar gives a good impression of the shape of the ice shelf at larger scales, its trace distance is large (10 m) and primarily registers nadir reflections. The narrow aperture thus provides only limited insight ~~in~~ into the precise geometry of the channel, especially steep structures like the flanks of the basal channel. In addition radar signals typically do not penetrate below wet ice-bed contacts, making it hard to determine the nature of subglacial material: is water exclusively present on hard bedrock or does the substrate also consist of sediments~~in which case we can expect recent sedimentation on the seabed~~?

To investigate the ice–bed, ice–ocean characteristics we deployed an active source, high-resolution seismic survey concentrated at an isolated surface and basal channel on the west side of the sheet–shelf transition of SFG (Fig. 1). The highly resolved seismic signal allows ~~to reconstruct~~ complex subglacial structures like basal channels ~~properly,~~ to be reconstructed given the larger aperture of the system compared to airborne radar. It also informs us about subglacial and ocean floor properties, as the signal penetrates through water containing substrata and the sub-shelf ocean cavity. This seismic survey~~is backed up~~ , collected in January 2017, is supported by airborne radar data of the sheet–shelf transition of SFG collected ~~in 2017.~~ later that month. Key questions we want to answer are: What initializes the surface and basal channel? How does it ~~proceed~~ continue upstream of the grounding line? Is there any active subglacial drainage connected to the channel?

We first discuss the survey site and the different data sets, then the results of the seismic data analysis. Finally, we discuss the possible interpretations of our findings~~, including subglacial landforms~~.

2 Survey area and data

2.1 Site description

SFG is an ice stream in ~~West~~ Antarctica feeding into the Filchner Ice Shelf. The ice stream lies between Foundation Ice Stream in the southwest (also grid southwest) and Recovery Glacier in the northwest~~(Fig. 1).~~ . The northward ice flow is ~~tugged in between the Pensacola Mountains~~ constrained between the Dufek Massif (the northern part of the Pensacola Mountains) on the western side and the Argentina Range on the eastern side constraining the ice shelf for 50 km ~~.~~ (Fig. 1). The drainage basin of SFG is ~~not that well~~ poorly defined (Rignot et al., 2011). Although it drains from interior East Antarctica, it is linked to

West Antarctica through the Filchner-Ronne Ice Shelf (Bingham et al., 2007). At the grounding line (GL) the ice is grounded 1200-1400 m below sea level (mbsl, WGS84 ellipsoid) with a surface velocity of 200 m/a. Upstream of the GL the bed is retrograde, it dips gently (slope of 0.28°) for some 20 km followed by a 400 m rise over the next 10 km and a fairly constant depth over the next 30 km (Fretwell et al., 2013). The survey target was ~~an isolated~~ a single and only surface channel (at the surface of the ice shelf) and its basal channel (at the base of the ice shelf) on the western side of SFG, not influenced by other basal channels which might affect the ice dynamics or ice–seawater interaction. At the GL we performed a high-resolution seismic reflection survey consisting of two ~~along- and three across-profiles forming a grid.~~ along-flow and three across-flow profiles (Fig. 1).

2.2 ~~Surface~~ Ice surface velocities and grounding line position

~~Surface~~ Ice surface velocities were combined from Landsat-8 and TerraSAR-X derived velocity fields. Landsat-8 velocity fields were downloaded ~~in near real time~~ from the Global Land Ice Velocity Extraction from Landsat 8 (GoLIVE) database (Scambos et al., 2016). Here preference was given to 64 day repeat passes as a trade-off between accuracy and decorrelation (Fahnestock et al., 2016). Due to orbital constrains Landsat velocity estimates reach a maximum latitude of ∼82.7°S which is just upstream of the grounding line of SFG (Figure 1a). In order to extend the velocities further south, we employed additional data takes from TerraSAR-X acquired in left looking mode. TerraSAR-X surface velocity fields were calculated by means of intensity offset tracking on single look complex imagery (e.g. Strozzi et al., 2002). Subsequently all velocity fields were filtered by the three step filtering procedure introduced by Lüttig et al. (2017) and merged into a continuous velocity mosaic. Employing the same TerraSAR-X data as in the calculation of the velocity fields we were able to generate several coherent double differential interferograms which were used to slightly modify grounding line locations (Fig. 1c) obtained from ~~DLR~~ the Deutsches Zentrum für Luft- und Raumfahrt (DLR) following well established methods (e.g. Rignot et al., 2011).

2.3 Airborne radar data

~~In~~ Late January 2017, the British Antarctic Survey (BAS) collected airborne ice-penetrating radar data with the PASIN2 system (an upgraded version of that described by ~~Rippin et al. (2014)~~Jeofry et al. (2018a). The radar acquired data with a repetition frequency ~~3125~~ of 312.5 Hz, which was then ~~pre-stacked~~ stacked and processed with an unfocused SAR algorithm before being decimated to an equivalent along-track spacing of ∼11 m. The onset of the ~~bed reflector~~ basal reflection was then obtained with a semi-automated process and merged with a laser surface terrain mapper to give the ice thickness and bed elevation: a wave speed in ice of 0.168 m μs^{-1} along with a 10 m firn correction was used.

2.4 Routing of subglacial water

To determine the subglacial water pathways we used a simple flux routing scheme to compute subglacial water pathways as described in Humbert et al. (2018). Subglacial water flow is governed by the hydraulic potential Φ (Shreve, 1972), which can

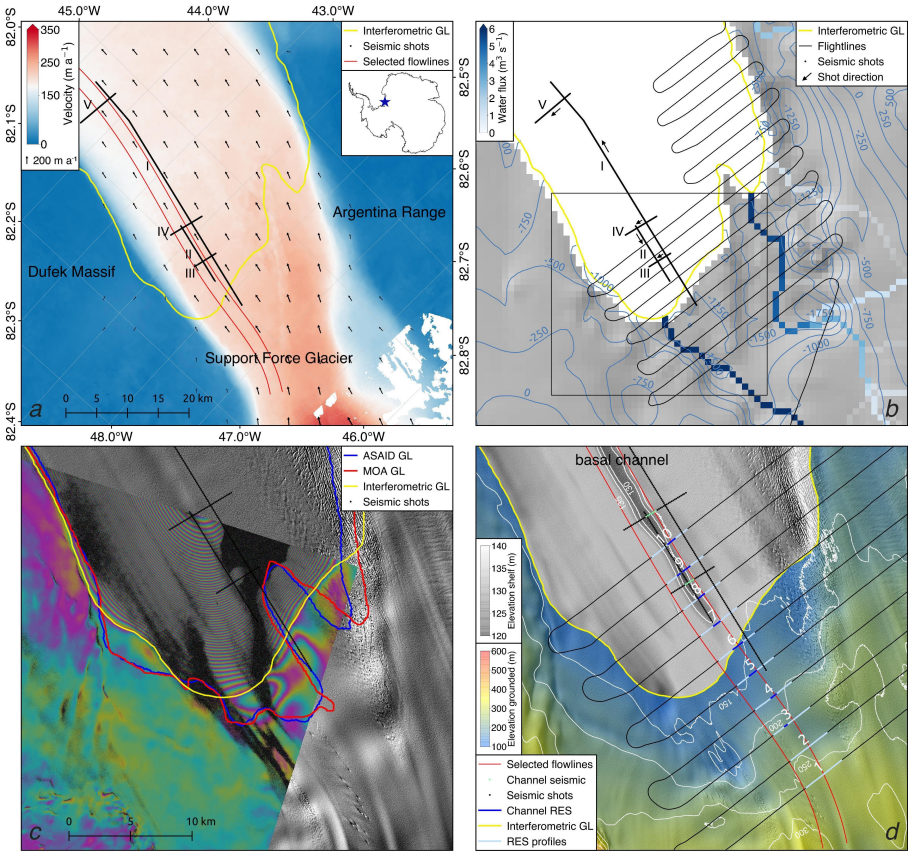

Figure 1. Location of the seismic and airborne radar ~~survey~~ surveys of the GL area of SFG. (a) ~~Surface ice~~ Ice surface velocity map of the survey area. The seismic ~~survey grid is~~ profiles are marked by black dots, ~~along-profiles~~ along-flow profiles I and II and ~~across-profiles~~ across-flow profiles III, IV and V. Two flow lines are marked in red and the GL in yellow. Inset: location of SFG in Antarctica. (b) Modeled subglacial water routing flux at SFG from the static hydrological potential. Shown are our updated bedrock compilation, a combination of BEDMAP2 and the collected airborne radar survey (thin black looping line). The shooting direction of the seismic profiles are shown by the arrows. The black rectangle marks the subregions of (b) and (c). (c) Three proposed GLs are marked in blue (ASAID Bindschadler et al. 2011), red (MODIS Scambos et al. 2007) and yellow (based on interferometry). The background is a shaded version of the 8 m Reference Elevation Model of Antarctica (REMA, Howat et al. 2019) overlaid by a TerraSAR-X interferogram used in the delineation of the grounding line. (d) The topography of the ice shelf (grey) indicates the surface channel. Numbered are loops 1 to 10 of the airborne radar data. Loops 1 to 5 are on the grounded part. Loops 7 to 10 represent the shelf, loop 6 is at the GL. In light blue we see the radar ~~across-profiles~~ profiles shown in Figure 4. In green (seismic profiles) and dark blue (radar) we see the shot locations at the ~~sub-ice~~ basal channel.

be written as

$$\Phi = \rho_w g h_b + \rho_i g H, \tag{1}$$

where ρ_w is the density of water, g acceleration due to gravity, h_b bed elevation, ρ_i density of ice and H the ice thickness.

Table 1. Properties of the ~~five~~ collected seismic profiles of SFG. Profile II is not listed here as it will not de discussed in the paper.

Profile	length (km)	Source	Direction~~Position from GL~~
I	43.5	10 m (100 g) detonating cord	along-flow~~3.90 km upstre~~
~~II10.010 m (100 g) detonating cordalong-flow3.50 km downstream of GL~~III	4.2	150 g cartridge in borehole	across-flow~~7.61 km down~~
IV	6.0	10 m (100 g) detonating cord	across-flow~~14.15 km dow~~
V	7.5	10 m (100 g) detonating cord	across-flow~~38.45 km dow~~

For the bed elevation h_b we used a combination ~~from~~ of BEDMAP2 (Fretwell et al., 2013) and the airborne radar data. The airborne radar profiles were nested into the BEDMAP2 dataset using the continuous curvature splines in tension algorithm implemented in the Generic Mapping Tools (GMT, Smith and Wessel, 1990). Next to our airborne radar data we incorporated all regionally available Operation IceBridge MCoRDS L2 ice thickness measurements collected in 2009 and 2014 in our analysis (Paden et al., 2019). In order to achieve a smooth transition between BEDMAP2 and the radar data we further included data points from the gridded BEDMAP2 dataset within a 50 km buffer in the interpolation.

The modeled water routing (Fig. 1b) shows expected subglacial drainage routes entering the ocean cavity of SFG. ~~In agreement with Alley et al. (2019), three~~ Three influx entrances are predicted at ~~the shear margins of SFG: two smaller ones~~ SFG: A smaller one and larger one on the eastern side and one larger influx on the western side, close to the surface channel and the seismic survey area. Our seismic survey focussed on the larger influx entrance on the western side of SFG with a predicted water influx of $190 \times 10^3 \mathrm{m}^3 \mathrm{a}^{-1}$.

2.5 Seismic data recording

~~In total~~ Early January 2017 we collected 71 km of seismic data divided over five profiles, numbered I to V ~~, forming a grid~~ (Fig. 1a, b). We used a 300 m snow streamer with 96 gimballed 30 Hz vertical compressional wave (p-wave) sensors, pulled behind a Nansen sledge carrying the recording equipment (four ~~Geodes~~ Geometrics GEODE units recording 24 channels each). The record length was set to 5 s and the sample ~~rate~~ interval to 0.5 ms. We used a snowmobile to pull the sledge and streamer between shot locations. As a source we mostly used 10 m detonating cord of 10 g/m (so each shot used 100g PETN) placed 34 m in front of the near offset geophone and parallel to the snow streamer. At ~~across-profile II~~ profile III we used 5 m deep drilled boreholes filled with 150 g pentolite cartridges. The shot spacing was half a streamer length, 150 m, resulting in single-fold data coverage. We refer to the single-fold data as profiles ~~and collected two along-profiles and three across-profiles~~ (Table 1). Profile II will not be discussed in the paper as it has a complex structure and hardly contributes to the paper.

During the data acquisition we collected 13 long offset gathers. At these shot locations we placed four shots of detonating cord at one location and recorded the shots at continuously decreasing offsets:

- Shot 1: offset 934 to 1234 m, streamer 934 m from the shot
- Shot 2: offset 634 to 934 m, streamer 634 m from the shot

- Shot 3: offset 334 to 634 m, streamer 334 m from the shot
- Shot 4: offset 34 to 334 m, streamer 34 m from the shot, profiling configuration

We used Shot 4 both in the long offset gather and for profiling. We created three types of processed data sets for the following applications:

- Profiles: Here the processing aim is to get an xz-image (x-axis: horizontal and z-axis: vertical) revealing the dimension and structure of the ice, ocean cavity and seabed. The data were band pass filtered (30–540 Hz), stacked, Kirchhoff time migrated and depth converted. Especially depth conversion of the time migrated profiles is important as the ~~sub-shelf~~ basal channel area has considerable topography over a relative flat seabed. As the seawater is a slow p-wave velocity layer, thickness variation in the water column induces time delays in the underlying seabed and an apparent seabed topography in the time migrated profiles.
- Single shot gathers to determine the seismic reflection coefficient R: Here the aim is to map the amplitude values of different subsurface reflections and of the direct wave of raw shot gathers. Except for adding a geometry, these shots were not processed as any processing affects the amplitudes.
- Long-offset gathers: Here we combine four shots with sequentially increasing offset into one shot location with a long offset. The aim here is to register the Normal Move Out (NMO) of a reflection for long offsets (time delay of a reflection with increasing offset) from which subsurface seismic p-wave velocities can be derived. The data were processed such that the reflections are best visible. Processing steps include muting, spiking deconvolution, band pass and fk-filtering.

2.6 Seismic reflection and transmission coefficient at normal incidence~~:~~

Reflectivity at a planar and specular two media interface in the subsurface depends on contrast of ~~P-wave~~ p-wave velocity (V_p), ~~S-wave~~ shear wave (s-wave) velocity (V_s), density (ρ) and the angle of incidence (θ) at the interface of the two considered media (Aki and Richards, 2002). At normal incidence the reflection coefficient R is solely determined by the contrast of the acoustic impedance ($Z = \rho V_p$) at the media interface:

$$R = \frac{Z_2 - Z_1}{Z_2 + Z_1} = \frac{\rho_2 V_{p_2} - \rho_1 V_{p_1}}{\rho_2 V_{p_2} + \rho_1 V_{p_1}}, \tag{2}$$

where subscripts 1 and 2 refer to upper and lower media. The θ-dependency of the reflection coefficient, $R(\theta)$, at a media interface can be expressed by:

$$R(\theta) = \frac{A_1(\theta)}{DA_0} r(\theta) e^{\alpha r(\theta)}, \tag{3}$$

with $A_1(\theta)$ being the amplitude of the primary reflection of the considered interface and A_0 being the source amplitude, D a directivity factor caused by the use of detonating cord as a source (when using point sources such as borehole shots $D = 1$),

$r(\theta)$ the distance of the primary wave and α the seismic attenuation coefficient. These quantities can all be determined from single shot records. The directivity factor D is discussed ~~below in the determination of A_0 subsection~~ in subsection 2.8.

With a target depth of 1400 m or deeper, and an offset ranging ~~of~~ from 33 to 330 m ~~, we get~~ ($0.6° \leq \theta \leq 6.7°$~~. Thus we approximate the considered~~), the reflections of the profiling shots are considered as being normal incidence. A shortcoming of using a relative small spread is that we are not able to plot the θ-dependency and perform an Amplitude-Versus-Angle (AVA) analysis of subglacial or seabed materials making identification less certain.

~~At normal incidence the reflection coefficient is solely determined by the contrast of the acoustic impedance ($Z = \rho V_p$) at the media interface:~~

$$R = \frac{Z_2 - Z_1}{Z_2 + Z_1} = \frac{\rho_2 V_{p_2} - \rho_1 V_{p_1}}{\rho_2 V_{p_2} + \rho_1 V_{p_1}},$$

~~where subscripts 1 and 2 refer to upper and lower media. In Table 2 we consider~~ Using the same values and lithology as Christianson et al. (2014) we calculated R at normal incidence (Table 2) from the following media interfaces we encounter in our survey area:

- grounded ice–bed interface;
- shelf ice–seawater interface;
- seawater–seabed interface;

In all cases of considered media interfaces, the acoustic impedance of the upper medium, ice (grounded or shelf ice) or the sub-shelf seawater can be estimated quite accurately as the material (ice or seawater) is known and the acoustic impedance of the lower medium (subglacial material or seabed) is unknown. Using both equations we can determine the acoustic impedance of subglacial material and the seabed ~~of~~ from single shots.

To calculate R at the seawater–seabed interface (R_{s-b}, where subscripts i, s and b refer respectively to ice, $seawater$ and bed (both the bed upstream of the GL and seabed), respectively) we assume normal incidence. The smallest possible value for R is caused by an ice–seawater transition; with $Z_i = 3.44 \times 10^6$ kg ~~/m^{2}s~~m^{-2}s^{-1} and $Z_s = 1.45 \times 10^6$ kg ~~/m^{2}s~~m^{-2}s^{-1} we get:

$$R_{i-s} = \frac{Z_s - Z_i}{Z_s + Z_i} = \frac{(1.45 - 3.44) \times 10^6}{(1.45 + 3.44) \times 10^6} = -0.41. \tag{4}$$

The transmission coefficient T is given by:

$$T = \frac{2Z_1}{Z_2 + Z_1} = \frac{2\rho_1 V_{p_1}}{\rho_2 V_{p_2} + \rho_1 V_{p_1}}. \tag{5}$$

To calculate R_{s-b} we must take into account the energy loss at the ice shelf–seawater interface. To compensate for this energy loss we assume normal incidence and an abrupt transition at the ice–seawater interface. Under these assumptions and with the ice–seawater transmission coefficient ($T_{i-s} = 1.41$) and seawater–ice transmission coefficient ($T_{s-i} = 0.59$) we get

$$R_{s-b} = \frac{A_1(\theta)}{A_0 T_{i-s} T_{s-i}} \frac{A_1(\theta)}{T_{i-s} T_{s-i} A_0} r(\theta) e^{\alpha r(\theta)} = \frac{A_1(\theta)}{0.83 A_0} r(\theta) e^{\alpha r(\theta)}, \tag{6}$$

Table 2. Ranges of R for different media contrasts at normal incidence. Top: If the upper medium Z_1 is ice. Bottom: If the upper medium Z_1 is seawater. The acoustic impedances and lithologies of the lower media Z_2 are similar to Christianson et al. (2014).

Media contrasts with ice:	R min.	R max.
Lithified sediments/bedrock	0.30	0.67
Consolidated sediments	−0.05	0.18
Unconsolidated sediments	−0.08	0.03
Dilatant till	−0.11	0.00
Seawater	−0.42	−0.39
Media contrasts with seawater:	**R min.**	**R max.**
Lithified sediments/bedrock	0.62	0.67
Consolidated sediments	0.35	0.55
Unconsolidated sediments	0.28	0.41
Dilatant till	0.25	0.38

with $A_1(\theta)$ being the amplitude of the seabed reflection.

2.7 Seismic attenuation of the ice and seawater

To determine the seismic attenuation α we need an estimate of the temperature of the shelf ice. We used temperature data from the 862 m long borehole FSW2 at the Filchner Ice Shelf at $-44.22546°$W, $-80.56532°$S, about 190 km downstream (northwest) of our survey area and another 275 km upstream from the calving front of the Filchner Ice Shelf. The installed thermistor chain showed an ice temperature range between –29°C at 10 m depth to –24°C at 650 m depth then increasing to –2~~.5~~.3°C at the base. As the ice shelf at the survey area is thicker (1300 m), we extrapolated the temperature curve~~giving and~~. Using this temperature profile, a center frequency of 100 Hz, V_p = 3750 m s^{-1} we calculated average seismic attenuation of 0.2 ~~/km~~km^{-1} for the entire ice column (Peters et al., 2012; Bentley and Kohnen, 1976).

We used the seawater temperature from the same borehole data, -2.3°C, to calculate the seismic attenuation of the water column. Assuming a constant temperature for the entire subglacial seawater column, we get an attenuation of 0.001 dB ~~/km~~km^{-1} (Ainslie and McColm, 1998). This converts to 1.15×10^{-4}~~/km~~km^{-1} which is so low that we can ignore this component.

~~Values of~~ With α of the ice and sea column known and Equations 6 and 3 we can calculate R~~for media contrasts we most likely encounter are listed in Table 2~~. In general, one can say that the higher the water content of the lower medium Z_2, the smaller is R (Table 2). If ice is the upper medium, the range of R is larger than if the seawater is the upper medium, making the interpretation of the seabed more sensitive to uncertainties. In general, R has the same trend i.e. the higher the water content of the seabed sediment, the smaller is R, but a distinction between subglacial unconsolidated or dilated till is not possible.

2.8 Determination of the source amplitude A_0

To determine A_0 we used the ~~method described by Holland and Anandakrishnan (2009) as the~~ direct path method (Holland and Anandakris
, whereby the amplitudes of primary reflections of geophone pairs with a travel path ratio of 2 are compared. It was not possible to employ the alternative multiple bounce method (Smith, 1997), as the primary multiple is hardly visible in the data. Assuming α does not change over the travel path, A_0 can be calculated. As our geophones are vertically orientated and the direct wave is a diving wave (a continuously refracted wave due to the continuous densification of the firn pack (Schlegel et al., 2019)), we used pairs of traces at larger offsets (97 m and larger) from the source which causes the ray-path of the diving wave to arrive at angles closer to normal incidence.

The detonating cord, placed in front of and parallel to the streamer, makes the source directional. ~~This~~ Detonation creates a wave front spreading cylindrically, perpendicular to the detonating cord orientation and semi-spherical at the ends of the cord. The cylindrically spreading wave front contains more energy and mostly agitates the subsurface whereas the spherically spreading wave front passes the streamer as a diving wave. This means we underestimate the source amplitude A_0 when using the direct path method.

At the ice–seawater interface, where the transition was abrupt, we determined A_0 by setting $R_{i-s} = -0.41$. At these transitions we know the acoustic impedance of the upper and lower media, namely ice and seawater, so here we can calibrate R_{i-s}. We refer to these shots as calibrated shots. Transitions from shelf ice to the seawater are not always acoustically abrupt, accreted ice or placelet ice may have formed at the base of the ice, giving (most often) ~~a larger value~~ larger values for R_{i-s} and $T_{i-s}T_{s-i}$. We considered ~~25~~ 26 shots (21 at ~~along-profile Iand 4 at the across-profiles~~profile I, one at profile III, two at profile IV and two at profile V) of which eight (six at ~~along-profile Iand two at the across-profiles~~profile I, one at profile IV and one at profile V) had an abrupt ice–seawater transition at the $\sim$ 9 m scale of vertical resolution. From these eight shots we derived the source amplitude A_0 reliably by setting $R_{i-s} = -0.41$ and compared this with A_0 derived from the direct path method. The direct path method underestimates ~~A_0 on average~~ A0 by a factor ~~,~~ of 2.6, equivalent to the directivity factor ~~,~~ ~~$D = 2.6$ ($2.1 \leq D \leq 3.1$)~~ D (2.1 < D < 3.1) from the cylindrically-spreading source. To compensate for the directivity of the source amplitude, we use DA_0 as the directionally compensated source amplitude as shown in Equation 3. The directionally compensated source amplitude has thus 19% ~~accuracy~~uncertainty.

Using DA_0 at five shots resulted in $R_{i-s} < -0.41$. As we assumed $R_{i-s} = -0.41$ is the smallest possible value for R, we set $R_{i-s} = -0.41$ at these shots and also refer to these as calibrated shots. With these additional calibrated shots we have a total of 13 calibrated shots (10 at ~~along-profile Iand 3 at the across-profiles~~profile I, two at profile IV and one at profile V) of the considered ~~25~~ 26 shots.

Based on the noise level preceding the primary reflection of the bed or seabed, we determined A_1 with 7% ~~accuracy~~uncertainty. This means we determined R_{s-b} of the calibrated shots with 7% ~~accuracy~~uncertainty. Of the remaining ~~12~~ 13 uncalibrated shots, where the directionally compensated source amplitude DA_0 has 19% ~~accuracy~~uncertainty, R_{i-b} and R_{s-b} could be determined with 32% ~~accuracy~~uncertainty.

3 Results and seismic interpretation

3.1 Seabed ~~artefacts~~depth conversion

In the following we will present time migrated and depth converted profiles. ~~An exception will be the comparison of along-profile II with along-profile I, where we will present time migrated profiles only.~~ Time migrated sections are not suitable to unravel the subglacial structure of the ~~seafloor~~ seabed when the ice shelf thickness shows significant variability over short distances. This is the case around the basal channel where the base of the ice shelf has significant topography and the ~~seafloor~~ seabed is fairly flat. As the seawater is a low velocity layer ($V_p = 1425$ m/s) in comparison to ice ($V_p = 3750$ m/s), the thickness variation of the ice shelf causes significant time variation in the ~~seafloor~~ seabed returns. The time migrated profiles show an apparent topography (an almost mirrored version of the topography of the base of the ice shelf) in the ~~seafloor~~ seabed caused by the different time delays of the ice shelf thickness. To derive the correct subsurface structure it is thus important to convert the migrated seismic profiles to depth. In general this works quite well but especially below the steep flanks of the basal channel the ~~seawater–seafloor contact~~ seawater–seabed morphology can not be properly recovered. ~~In other words, the structure of the seafloor is~~ The apparent morphology of the seabed is thus influenced by the topography of the ice shelf.

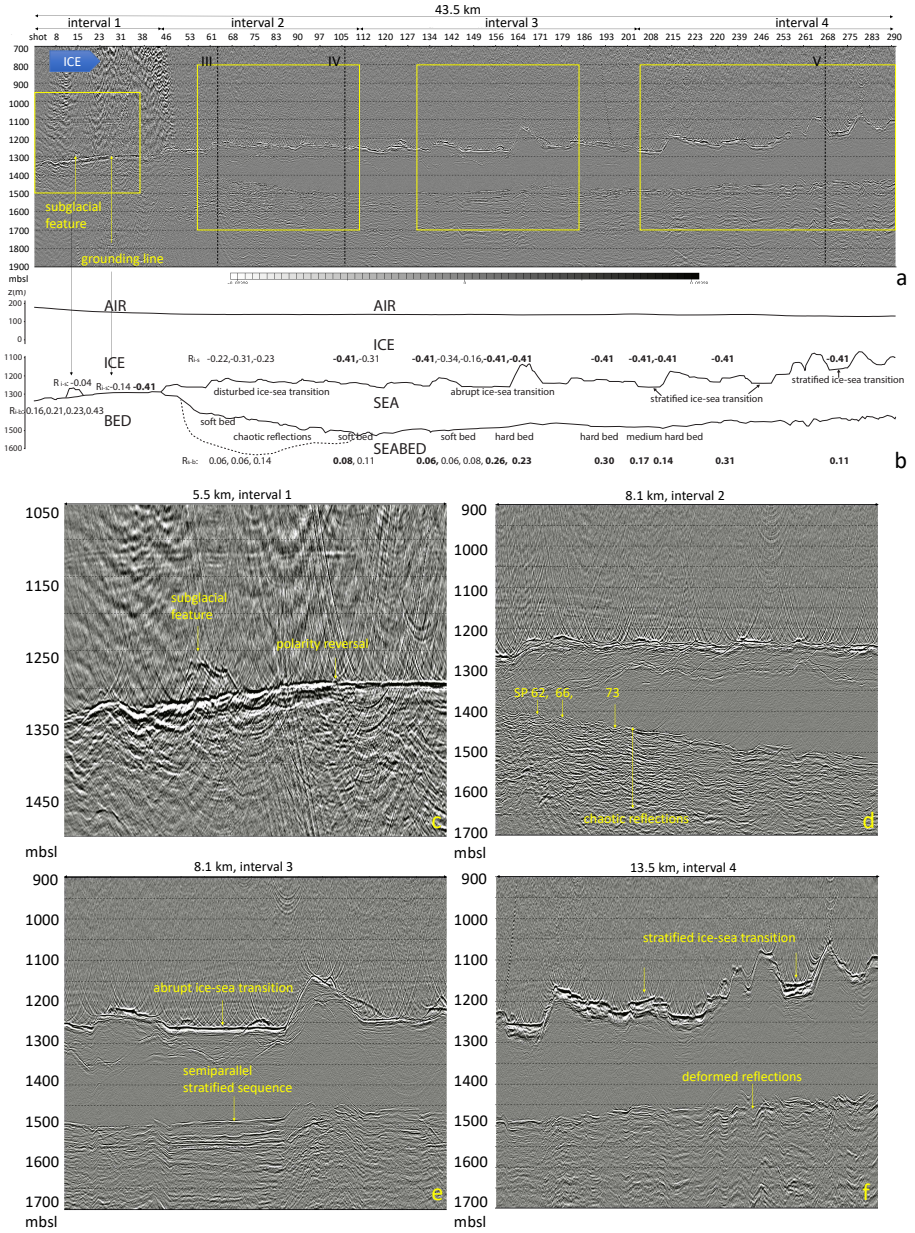

Figure 2. ~~Top:~~ Profile I, its schematic diagram, and four zooms showing the discussed characteristics. (a) Time migrated and depth converted ~~(800 m to 2000 m)~~ seismic ~~along-profile~~ profile I. The ice flow is from left to right~~, the x-axis indicates the shot~~. Shot point (SP) ~~location and~~ numbering is ~~divided~~ along the x-axis, increasing in ~~four intervals~~shooting direction. The ~~first 3.9 km are grounded ice then transitioning~~ profile is divided into ~~an ice shelf. We identify~~ four intervals marked by the ~~GL at SP 26 where~~ double headed arrows above the ~~polarity of~~ profile. The yellow frames represent the ~~ice base reflection switches from positive~~ four zooms shown at figures (c) to ~~negative~~(f). The crossings of ~~the three across-profiles~~ profiles III, IV and V ~~,~~ are marked by the black dashed lines. ~~Bottom:~~ (b) A schematic ~~representation~~ diagram of ~~the seismic~~ profile ~~above~~ I marking the boundaries of the ice surface~~and~~ , base and the seabed. ~~Clearly marked on the base of grounded ice is a subglacial drainage feature.~~ The ~~values of the~~ calculated reflection coefficients R are shown at their position. The bold numbers represent calibrated shots and the normal numbers uncalibrated shots.(c) Zoom of interval showing the polarity reversal of the base at SP 26 and the subglacial feature at the flat bed. (d) The $\sim$ 200 m thick sequence with ~~$R_{i-s} = -0.41$~~ chaotic reflections and ~~R_{s-b}~~ little signal loss of the seabed marked by the dashed line in b. The seabed has ~~7% accuracy~~reversed polarities at SP 62, 66 and 73. The transition

3.2 Seismic ~~along-profile~~ profile I

The ~~top of Figure 2 shows~~ first 3.9 km of the 43.5 km long ~~seismic along-profile I crossing the GL~~ profile I (Fig. 2a) are grounded ice. The GL is at shot point (SP) ~~26. The bottom of Figure 2 shows its schematic lay out with calculated values for R~~26 where the polarity of the ice base reflection reverses. There are ten locations where $R_{i-s} = -0.41$ and the shots are calibrated (Fig. 2b), six where the ice–seawater transition was abrupt and we calibrated $R_{i-s} = -0.41$ and four locations, SP 208, 209, 231 and 273, where $R_{i-s} < -0.41$ and was set $R_{i-s} = -0.41$. Based on the topography, structure and the reflectivity of the ice-base contact and seabed contact, we distinguish four intervals in ~~along-profile~~ profile I.

Interval 1 is from SP 1 to SP ~~44.~~ 44 (Fig. 2 a and c). We see a flat bed in direct or close contact with overlying ice. The bed starts at 1350 mbsl at SP 1, rising to 1300 mbsl at SP 26 after which the bed stays at 1300 mbsl to SP 44. The polarity of the ice–bed contact of the grounded ice~~is positive from SP 1 to SP 26, after which the polarity changes to negative~~ , we refer to in this paper as positive, reverses (becomes negative) after SP 26 and stays like that for the rest of the profile. The location of the polarity change ~~, SP 26, corresponds to the position~~ is within 150 m of the GL derived by interferometry ~~.~~ (Fig. 1c). From SP 4 to SP 22 ~~the reflection coefficient~~ R_{i-b} increases from 0.16 to 0.43. From SP 26 to SP 44, R_{i-s} is negative and decreases from -0.14 at SP 30 to -0.41 at SP 33. The ice is ~~uncoupled~~ floating but the thickness of the seawater column is too small to be made out.

At the base of the grounded ice, between SP 11 and SP 17, there is an elongated feature that appears to lie on a harder flat bed . It is approximately 50 m high and 1200 m long and ~~has a small negative reflection coefficient ($R = -0.04$)~~ $R = -0.04$ at the ice bed contact. Our subsequent analysis shows this feature likely has evidence of ~~subglacial drainage~~ a subglacial drainage channel and hereafter will be referred to as the subglacial ~~drainage~~ feature.

Interval 2 is from SP 44 to SP ~~110.~~ 110 (Fig. 2 a and d). The ice–seawater contact, the base of the ice shelf, lies between 1220 to 1300 mbsl, has minor topography with ~~anticlines~~ concave cavities 20 to 50 m above the surrounding base, and has R_{i-s} values varying between ~~$R_{i-s} = -0.22$ to $R_{i-s} = -0.41$~~ $-0.41 \leq R_{i-s} \leq -0.22$. The ice–seawater contact is ~~likely~~ not abrupt, as the transition appears as an approximately 20 m sequence ~~of discontinuous reflections.~~ with chaotic reflections. This gradual ice–seawater transition probably leads to an increased energy loss and subsequently a larger (so less negative) R. At SP 44 the ocean cavity ~~deepens as the seafloor~~ thickens as the seabed starts descending steeply to 1400 mbsl at SP 55 and then dips more gently to 1500 mbsl at SP 110. The polarity of the ~~seafloor contact initially is~~ seabed contact is initially small and positive but occasionally, at SP 62, 66 and 73, negative. Between SP 55 and SP ~~110 the seafloor~~ 107 the seabed consists of a ~8 km long and ~200 m thick ~~, transparent, stratified but disturbed sequence with~~ sequence with chaotic reflections and little signal loss with increasing depth (hereafter referred to as the sequence with chaotic reflections). R_{s-b} ~~varying~~ varies between $0.06 \leq R_{s-b} \leq 0.14$. Downstream of SP ~~110~~ 107 the character of the ~~seafloor~~ seabed gradually changes to ~~less stratified but still transparent~~a stratified sequence having less semiparallel, high amplitude, reflections.

Interval 3 lies between SP 110 and ~~204.~~ 204 (Fig. 2 a and e). The ice–seawater contact lies mostly between 1230 and 1260 mbsl~~and consists of~~ , is (semi)~~horizontal terraces interchanged with anticlines~~ horizontally terraced interchanged with concave cavities 50 to 150 m above the surrounding base, reaching 1140 mbsl at SP 164. The ice–seawater contact is more abrupt,

especially in the lower (semi) horizontal terraces (SP 145 to SP 160 and SP 171 to SP 180). The ~~seafloor is transparent but less stratified with~~ seabed consists of a stratified sequence having less semiparallel, high amplitude, reflections, hereafter referred to as the stratified sequence with semiparallel reflections, and an increasing acoustic hardness downstream from $R = 0.06$ at SP 130 to $R = 0.3$ at SP 191. This harder, ~~less stratified but transparent bed~~ stratified sequence with semiparallel, reflections can best be observed between SP 145 and SP 160.

Interval 4 lies downstream of SP ~~204.~~ 204 (Fig. 2 a and f). The seawater–ice contact now rises from 1270 to 1100 m, ~~has less (semi)horizontal terraces and more anticlines~~is less terraced and has more concave cavities. The ice–seawater transition at the terraces is no longer abrupt but a 20 to 30 m stratified sequence of ~~parallel~~ semiparallel reflections. This is especially visible in the lower terraces (SP 204 to SP 212, SP 243 to SP 250 and SP 269 to SP ~~270~~276). At this interval the ice–seawater transition has been set to $R = -0.41$ (SP 273) because the calculated $R < -0.41$. At the ~~seafloor~~ seabed R ($0.11 \leq R \leq 0.31$) is quite variable, larger then the second interval (SP 44–110) but not consistently high as in the third interval (SP 110–204).

~~Time migrated along-profiles II (a) and part of I (b). Both profiles are 10 km long, starting 4 km upstream of across-profile III. Along-profile II is recorded on the western flank of the sub-ice channel (Fig. 3) and as a result has two events from ice–seawater reflections (see arrows). (a) The first one at 0.63 s (marked with arrow) represents the top of the sub-ice channel (channel roof) and the second one at 0.7 s represents the ice shelf west of the sub-ice channel (base). The sub-shelf structure is influenced by the seawater column thickness but we can pinpoint the seabed in the basal channel (yellow arrow) based on across-profiles III and IV, marked by the black dashed lines. The seabed has some stratification but this sequence is significantly less thick then along-profile I shows. (b) A 10 km time migrated section of along-profile I. In order to compare the section with (a) it has not been depth converted as in Figure 2.~~

3.3 ~~Seismic along-profile II~~

~~We recorded along-profile II at the base of the surface channel. The profile is 10 km long starting 3.5 km downstream from the GL. Figure **??** compares the time migrated along-profile II with a time migrated part of along-profile I of the same length (10 km). Both profiles intersect across-profiles III and IV at the same distance. At along-profile II the surface channel (on the surface) is not in perfect hydrostatic equilibrium, it is somewhat offset to the west with respect to the basal channel. Consequently, we recorded along-profile II over the western flank of the basal channel (Fig. 3) . As a result the profile shows two events of the ice shelf–seawater contacts: one corresponds to the top of the basal channel, hereafter referred to as the roof, and the later one corresponds to the base west of the basal channel, hereafter referred to as the base of the ice shelf. For clarity the roof and the base of the basal channel and seabed returns have been marked. Depth conversion of the time migrated stack would obscure the seabed.~~

~~Contrary to along-profile I (Fig. **??**b) where the seabed consists of a 200 m thick stratification sequence between SP 60~~ Despite the seabed being migrated and ~~87, at along-profile II (Fig. **??**a), the seabed shows little sign of a stratification sequence in the basal channel. There is approximately 50 m of stratified material in the seabed between SP 50 and 42.~~ depth converted it (SP 250–291) shows apparent morphology: the deformed reflections are influenced by the the concave cavities of the ice–seawater transition.

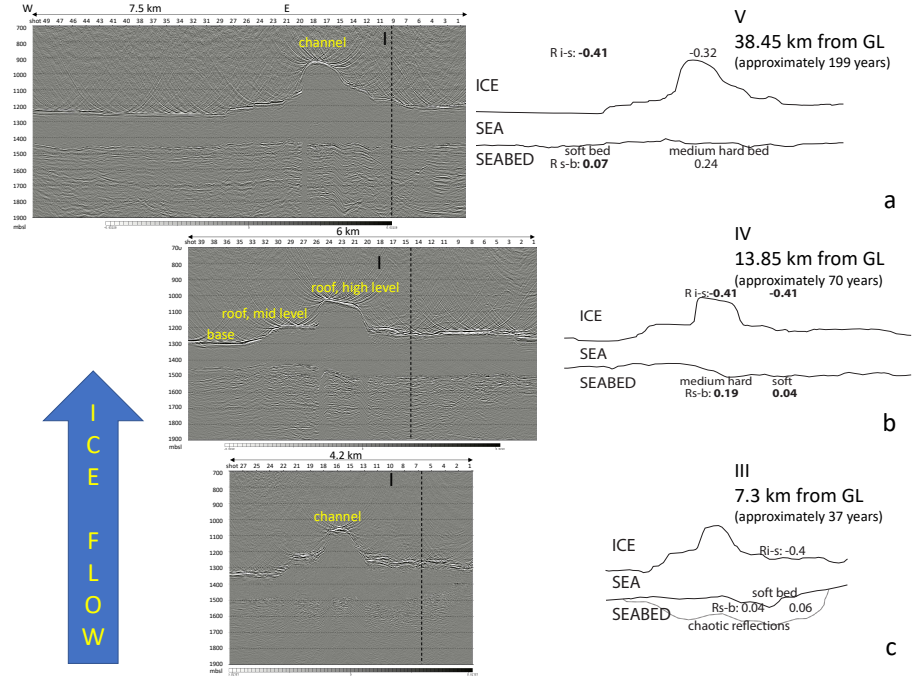

Figure 3. ~~Three across-profiles in along-flow sequence to show~~ Profiles III, IV and V, and their schematic diagram, showing the development of the ~~sub-ice~~ basal channel~~with the most upstream profile, along-profile III,~~ . The calculated reflection coefficients (bold represents calibrated shots) are shown at their position in the ~~bottom~~diagram. The ice flow sequence is from bottom to top. The ~~crossings~~ crossing of the ~~along-profiles~~ profile I ~~and II are~~ is marked by the black dashed lines. The distance from the GL and the time lap for the ice to reach this distance ~~are~~ is mentioned on the right side. The ~~across-profiles~~ three profiles have been aligned across-flow with respect to the most westerly flow line of Figure 1a. ~~As a result the crossings of the along-profiles (black dashed lines) shift slightly westward with flow. (~~a) The most downstream ~~across-profile~~ profile V, with the high-level roof of the channel marked. (b) ~~Across-profile~~ Profile IV, for clarity the high and mid-level roof of the channel as well as the base are marked. (c) The most upstream ~~across-profile~~ profile III. The sequence with chaotic reflections is marked in the schematic diagram by the dashed line.

3.3 Seismic ~~across-profiles~~ profiles III, IV and V ~~Figure 3 shows the three time migrated and depth converted across-profiles downstream of the GL. At across-profile III~~

At profile III (Fig. 3) we used charges in 5 m deep boreholes whereas ~~across-profiles~~ profiles IV and V were recorded with detonating cord. The borehole charges produce a ghost with 5 – 7 ms delay, not present when using detonating cord at the surface. ~~In other words,~~ This causes the source wavelet of the borehole charges is longer as with detonating cord charges. As a result, the ice–seawater and seawater–seabed contacts of ~~across-profile~~ profile III are not as well resolved (they appear more stratified) as for ~~across-profiles~~ profiles IV and V.

~~A schematic comparison of the ice shelf development around the basal channel derived from the three seismic across-profiles in Figure 3. The ice flow is into the page. All 3.75 km long sections have been lined up against the most western flow line of Fig.1a. Vertically, they are positioned with respect to the ice shelf surface so that the ice thickness can be compared. (a) Comparing across-profile IV (dashed line) with V (continuous line). (b) Comparing across-profile III (dashed line) with IV (continuous line).~~

The basal channel on all three ~~across-profiles is terrace-shaped~~profiles is terraced, especially on the western side where the channel has a mid- and a high-level roof, ~~as indicated in Figure 3b. On across-profiles~~ (Fig. 3b). On profiles III and IV, the lower level of the ice shelf base lies at ~~app~~ 1330 mbsl and the roof of the basal channel, at 1050 mbsl. At ~~across-profile~~ profile V the character of the channel roof is more rounded but the terraces can still be made out. The base lies at 1250 mbsl and the high-level roof of the ~~sub-shelf~~ basal channel at 920 mbsl.

The seabed at the ~~across-profiles~~ profiles lies between 1450 mbsl and 1500 mbsl ~~, where we have to keep in mind that~~ (Fig. 3), but the migration and depth conversion (and thus ~~topography~~the morphology) of the seabed under the steeper flanks of the ~~sub-shelf~~ basal channel, is not correct. Especially across-profiles IV and V have a flat seabed that only shows some ~~"apparent " topography~~ apparent morphology under the steeper flanks of the ~~sub-shelf channel. The across-profiles show a thicker stratified sequence under the sub-ice channelwhich extends to the eastern side on across-profile III.~~ basal channel.

~~To see the development of the lateral position and the changing geometry~~ Profile III crosses the ~200 m thick sequence with chaotic reflections of interval 2. The seabed shows this sequence is 3.5 km wide and present under the basal channel, extending and increasing somewhat in thickness east of the basal channel~~, Figure 6 compares three 3.75 km long schematic sections derived from the seismic across-profiles in sets of two (section III with IV and section IV with V) . From~~ . The sequence is absent on the eastern and western sides (start and end) of across-profile III~~to IV (Fig. 6b), the terrace shaped multi leveled roof of the channel form stays preserved but widens from some 780 m to 920 m, rather than that~~ . At SP 11 the sequence has $R_{s-b} = 0.04$ and we know that at the crossing (SP 7) with profile I the sequence has $R_{s-b} = 0.06$. At profiles IV and V the ~~ice shelf thickness changes. The flanks of the basal channel become steeper but the height does not change noticeably although there may be some lowering in the center of the basal channel. From across-profile IV to V (Fig. 6a) , the terrace shape of the basal channel becomes less pronounced and the base is shallower. The flat roof of the channel becomes more rounded and the lower level roof on the western side, less pronounced. As the base is shallower, the ice shelf at across-profile V is thinner. Based on the flow line orientation the channel has moved westward in the downstream direction.~~ seabed below the basal channel has $R_{s-b} = 0.19$ and $R_{s-b} = 0.24$

3.4 ~~Basal~~ Radar images of basal channel~~characteristics in ten radar across-profiles~~

We selected ten ~~across-profiles~~ airborne radar profiles separated by 2.6 km in along-flow direction (Fig. 4) ~~. These track the basal channel andthe landform shaping the channel~~ tracking the basal and, upstream of the GL, the subglacial channel (the feature between the ice and bed upstream of the ~~GL. The~~ basal channel, probably water filled). They are ~3.75 km long~~radar profiles are shown in light blue and the basal channel and the landform shaping it upstream of the GL (hereafter referred to as landform) in dark blue in~~ , and their numbering corresponds to Figure 1d. The radar profiles are rotated 5° ~~SW–NE~~

counterclockwise with respect to the seismic ~~across-profiles~~across-flow profiles. Profile 10 ~~lies 10.85~~ is 10.9 km downstream of the GL, profile 6 is at the GL (partly grounded and partly at shelf), and profile 1 ~~lies 12.83~~ is 12.8 km upstream of the GL. ~~The~~

In Figure 5 we combine the basal reflection of the ice ~~is marked in blue.~~ of the ten migrated radar and the three seismic profiles in a schematic diagram to track the development of the subglacial channel and basal channel along its flow line. All 3.75 km long profiles have been lined up against the westernmost flow line of Fig.1a. The resolution of the radar data is not as good as that of the seismic data, so the shape of the basal channel can not be reconstructed as well~~. Nevertheless,~~, nevertheless, we can track ~~the basal channel and~~it. On the grounded ice we can track the subglacial channel at profiles 3, ~~upstream of the GL, landform up to radar profile 3, at least 7.7 km upstream of the GL after which the landform becomes indistinguishable from the bed.~~4, 5 and 6 where it increases in size from hardly distinguishable from the surrounding bed to 280 m at profile 6 at the grounding line and continues as a basal channel under the ice shelf. The basal channel meanders up to profile 9 after which the three remaining profiles 10, IV and V show a consistent migration westward. The height of the subglacial and basal channel is hard to determine accurately, partly because of the poorer resolution of the radar profiles but also because it is hard to determine what the base of the ice shelf exactly is so the heights should be seen as an indication rather then an exact measurement. In general the height of the basal channel is constant between profiles 7 and IV and then increases its height to 205 m.

To see the changing geometry of the basal channel, we restrict ourselves to the migrated, depth converted seismic profiles that reproduce the shape of the basal channel more accurately than the radar profiles (Fig. 6). From profile III to IV (Fig. 6a), the terraced multi leveled roof of the channel stays preserved but widens from some 780 m to 920 m, rather than that the ice shelf thickness changes. The flanks of the basal channel become steeper but the height does not change noticeably although there may be some lowering in the center of the basal channel. From profile IV to V (Fig. 6b), the terraced basal channel becomes less pronounced and the base is shallower (i.e. the ice shelf is thinner). As a result profile V moved upward. The basal channel also moved westward with respect to profile IV so in a downstream direction. The flat roof of the channel becomes more rounded and the lower level roof on the western side, less pronounced.

4 Discussion

4.1 The grounding line position

~~In Figure 1c three GLs are shown: in red MOA (Scambos et al., 2007), in blue ASAID (Bindschadler et al., 2011) and in yellow a GL we derived from interferometry. At along-profile~~ At profile I the polarity of the basal reflection ~~switches~~ reverses from positive to permanently negative in downstream direction at SP ~~26.~~ 26 (Fig. 2a). As negative polarity indicates the presence of water at the base, this ~~confirms~~ suggests the ice uncouples from the bed. Between SP 30 and 33 we see a decrease in R from $R_{i-s} = -0.14$ to $R_{i-s} = -0.41$ which is probably caused by an increase in water content in the subglacial bed. At SP 33 the ice is in contact with the seawater. We recorded SP 26 at 17:06 UTC, January 1, 2017. According to five GPS stations 13 km downstream from the GL, this is 3.5 hrs after high tide at which time there was 1.5 m additional uplift on a tidal range of 2.6

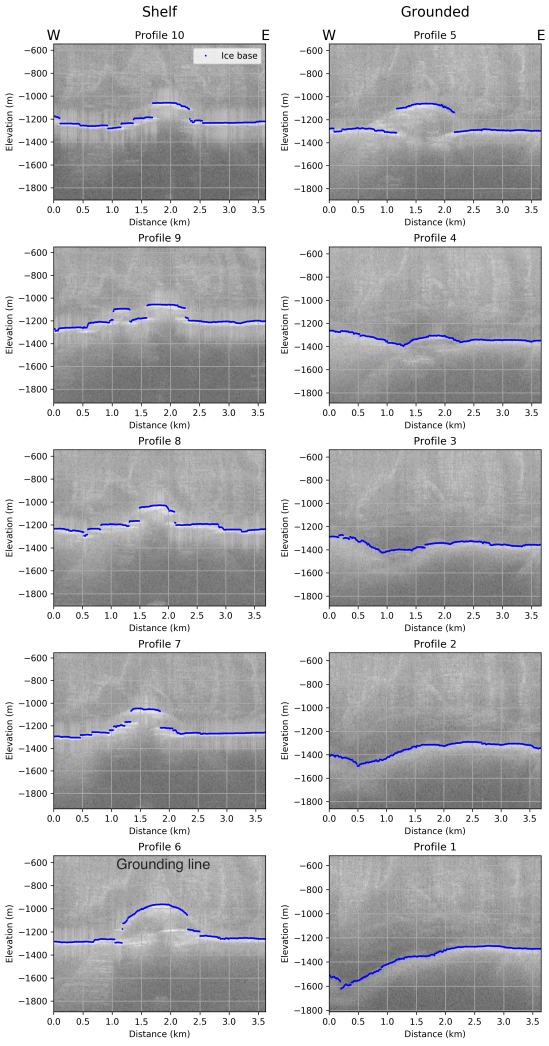

Figure 4. Return power, grey-scaled and depth converted radar profiles 1 to 10. Figure 1d shows their position. The ice flow direction is from bottom to top, starting with profile 1 (upstream) at the lower right corner up to 10 (downstream) in the upper left corner. The semi-automatically picked basal reflection (seawater and bed) of the ice is marked in blue. At profiles 1 to 5 the ice is grounded, profile 6 is at the grounding line and at profiles 7 to 10 the ice is floating.

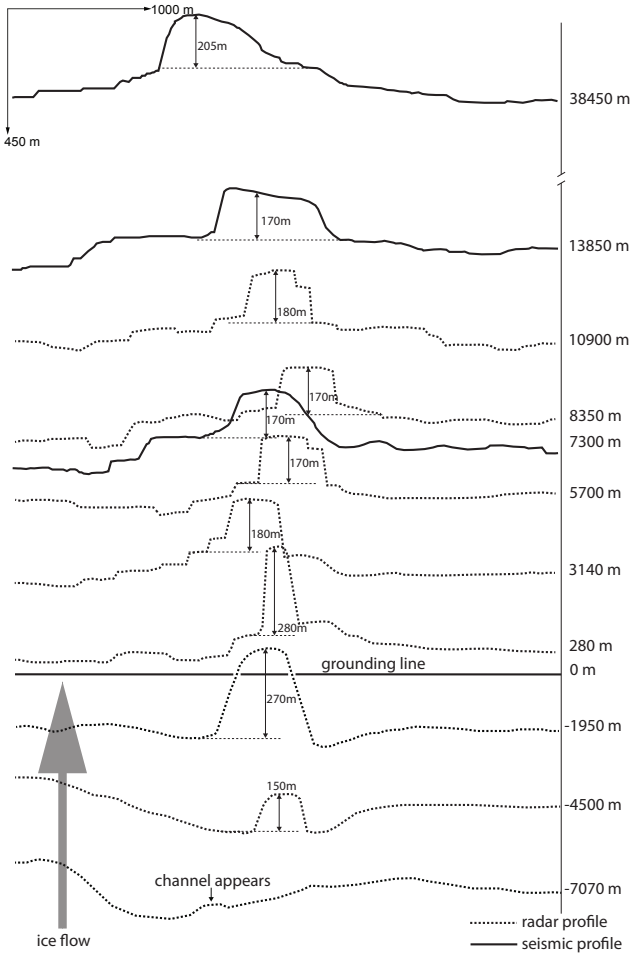

Figure 5. A schematic diagram of the shape and development of the subglacial channel under the grounded ice and basal channel under the ice shelf. The scheme combines the migrated radar (dashed) and seismic (continuous) profiles. The vertical axis shows the distances to the grounding line measured along the westerly flow line of Figure 1d.

m. As SP 26 ~~corresponds well with~~ lies within 150 m of the GL derived from interferometry ~~and not with the GL derived from the surface slope (MOA)~~ we refer to the GL as the one provided by interferometry in the remainder of the paper.

4.2 The structure of the ice shelf and ocean cavity

Looking at the structure of the ice sheet at the GL area of ~~along-profile~~ profile I (Fig. 2), we see an almost constant ice thickness gradient when the ice, initially flowing over a flat bed, passes the GL. Unlike the classic picture of the sheet–shelf transition, where rapid ice shelf thinning close to the GL causes a steeply rising ice shelf base, the sheet–shelf transition of SFG seems to be a mirrored version of this: SFG has a steeply descending ~~seafloor~~ seabed at SP 44 and an almost constant ice thickness

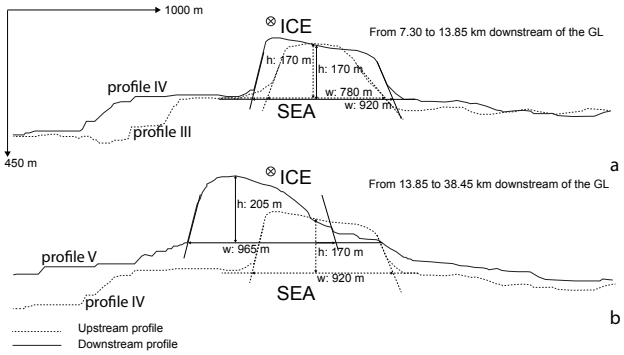

Figure 6. ~~Return power, grey-scaled and depth converted radar~~ A schematic diagram of the ice shelf development around the basal channel derived from the three seismic across-flow profiles ~~1 to 10.~~ in Figure ~~1d shows their position~~3. ~~The ice flow direction is from bottom to top~~Vertically, ~~starting~~ they are positioned with respect to the ice shelf surface so that the ice thickness can be compared. (a) Comparing profile ~~1~~ III (~~upstream~~dashed line) ~~at the lower right corner up to 10~~ with IV (~~downstream~~continuous line)~~in the upper left corner~~. ~~The basal reflection~~ (~~seawater and bed~~b) ~~of the ice is marked in blue. At profiles 1 to 5 the ice is grounded,~~ Comparing profile ~~6 is at the grounding~~ IV (dashed line~~and at profiles 7 to 10 the ice is floating~~) with V (continuous line).

downstream of the GL. This steeply descending ~~seafloor~~seabed, the onset of the ocean cavity, probably determines the GL position. The ~~lacking~~ absence of an ocean cavity at the flat ice shelf base upstream of SP 44 confirms this.

Generally we would expect the highest melt rates at the deepest part of the ice shelf, the GL, as that is where the melting point is lowest due to the pressure effect of the ocean. The topographically constrained ice flow, confirmed by the parallel flow lines (Fig. 1a) and the flat ice shelf base, allow us to use the ice thickness gradient as a first order approximation for basal melt (Fig. 2). As the base of the ice shelf is initially flat, any topography in the base is likely to be caused by basal melt. The constant ice thickness gradient of the ice passing the GL suggests there is little basal melting at the GL of SFG.

Once in contact with the ocean cavity at SP 44, there is some basal melting as the base of the ice shelf has some topography but this increases in downstream direction as we see an increase in the number of and the magnitude of ~~anticlines~~ concave cavities in the ice base. Interval 2 has some topography but small compared to interval 3 and 4. Interval 3 has one pronounced ~~anticline~~ concave cavity at SP 164 interchanged with lower terraces and interval 4 has several pronounced ~~anticlines~~concave cavities, at SP 215 and downstream of SP 250, interchanged with lower terraces. Dutrieux et al. (2014) observed a similar ice shelf geometry and attributed the terrace shaped structure to a steplike thermohaline ocean structure causing organized melting.

That there is little melting at the GL increasing in downstream direction is also confirmed by the seismic ~~across-profiles~~ profiles of Figure 6b. The ice shelf base of ~~across-profiles~~ profiles III and IV does not change much in depth but the basal channel itself widens. At Pine Island Glacier this channel widening was ascribed to ice dynamics, i.e. convergence at ice shelf surface and divergence at ice shelf base (Dutrieux et al., 2013; Vaughan et al., 2012). At SFG we observed no noticeable ice convergence at the surface channel, at least not distinguishable from the noise level. Between ~~across-profiles~~ profiles IV and V

we observe a general thinning of the ice shelf, both, above the ~~sub-ice~~ basal channel and outside of it. ~~Across-profile V crosses along-profile~~ Profile V crosses profile I in interval 4 where there is increased basal melting of the ice shelf.

4.3 ~~Characteristics~~ Properties of the ~~subglacial drainage feature~~seabed

At ~~along-profile I , below the grounded ice between SP~~ profile I we recorded 10 calibrated and 11 ~~and 17, the subglacial drainage feature appears to lie on a harder flat bed. It is unclear whether the subglacial drainage feature lies at nadir or off-nadir direction. Depending on this we have two possible interpretations:~~

~~Cross section of the seismic recording geometry of along-flow profile I during shots 11 to 17. The shooting direction and ice-flow direction are into the page, perpendicular to the cross section. The continuous and dashed black lines form the ice base derived from radar profiles 5 (continuous and greyscale image in figure) at the GL, and 6 (dashed) 2.6 km upstream from the GL. The landform at off-nadir direction is pointed out. The red semicircle represents the dimensions of a hypothetical subglacial drainage feature at nadir (50 m high, 1200 m long). The circular wave front reaches the base at nadir and the landform shaping the shelf channel at the same time.~~

~~1) If the seismic event is from off-nadir, we most likely recorded the top of the landform shown in Fig. 7. The schematic cross section shows the recording geometry of SP 11 to 17 from along-flow profile I. The ice base, showing the landform, comes from dashed profile 5~~uncalibrated shots. At the calibrated shots we will use R, ~~2.6 km upstream of the GL, and continuous to radar profile 6 at the grounding line. The spherical wave front, represented by the dashed circular line, reaches the off-nadir landform before the bed at nadir. In this scenario reflection coefficient $R_{i-b} = -0.04$ but $\theta = 45°$, so we need to consider the angle dependency of~~ having 7% uncertainty, for interpretation. At the uncalibrated shots where R ~~. Although the amplitude may be~~ has 32~~% accurate, the polarity is not affected by this uncertainty. For subglacial consolidated to unconsolidated sediments, $R < 0$ becomes smaller with increasing θ. So, if the event is from off-nadir, then the the landform consists of sediments having some degree of consolidation.~~

~~2) If the seismic event is from nadir, it would be a separate drainage feature on a hard bed, 1200 m long and approximately 50 m high, its dimensions represented by the red semi-circle in Fig. 7. The reflection coefficient $R_{i-b} = -0.04$ at normal incidence indicates that the subglacial material would consist of unconsolidated water containing sediments. So if originating from nadir, the subglacial drainage feature most likely is a stand alone subglacial conduit on a hard flat bed transporting wet sediments which are deposited at the downsloping seafloor, and the seismic event is not related to the landform and surface channel.~~

~~Both interpretations have consequences for the seismic acoustic velocity model and the resulting profile structure, because the subglacial drainage feature has a significantly lower V_P (1900 m/s) than ice (3750 m/s). If interpretation1 is correct, i. e. the subglacial drainage feature is off-nadir and is in fact the top of the landform, ice alone covers a hard flat bed. In that case the velocity model consists two layers: a top layer representing ice and a lower layer representing the subglacial flat hard bed. If interpretation 2 is correct, i.e. the subglacial drainage feature is nadir and a stand alone conduit on a hard flat bed, there would be a low velocity layer (the subglacial drainage feature) in between the ice and the hard flat bed. In that case the velocity~~

model has three layers: a top layer representing ice, a second layer representing unconsolidated, water containing sediments and a third layer representing the subglacial flat hard bed.

The two versions of the time migrated, depth converted profiles using either velocity model are shown in Figure **??**. If the subglacial drainage feature is off-nadir and in fact the top of the landform, we use the two-layer velocity model. The bed of the time migrated, depth converted profile, stays flat which agrees with both radar across-profiles that show no topography below along-profile I. If the subglacial drainage feature lies nadir, and we are dealing with a stand alone subglacial conduit, we use the belonging three-layer velocity model. The hard bed of time migrated, depth converted profile is no longer flat. Below the subglacial conduit the hard bed has a local rise. On an otherwise featureless bed, this is possible, but coincidental. Next to this, both radar profiles are featureless apart from the off-nadir landform. A 50 m high, 1200 m long subglacial conduit, as represented by the red semi-circle, would show up on the radar profiles unless this feature is so local that it does not cross the 2.6 km separated radar profiles. That is possible but again, would be coincidental.

Top: A zoom of the the subglacial drainage feature on a hard flat bed of the unmigrated along-profile I, also named stack. The negative polarity along the subglacial drainage feature clearly shows up. Bottom: Two time migrated and depth converted zooms, showing the effect on the underlying hard bed of the subglacial drainage feature, depending on wether we use a two-layer velocity model when the feature is off-nadir direction (lower left: interpretation 1), or a three-layer velocity model if the feature is nadir (lower right: interpretation 2).

Because of these two argumentations we prefer interpretation 1: the subglacial drainage feature is off-nadir and is in fact the top of the landform. With $R_{i-b} = -0.04$ and $\theta = 45°$ the bed most likely consists of sediments but the degree of consolidation is difficult to determine. This conclusion is based on the reflectivity of the off-nadir reflection of SP 11–17. As we lack a proper seismic across-profile over the landform, we can not retrieve its full structure. It may be that only the surface of the eastern side of the landform causing the reflection, consists of sediments and the deeper part bedrock.

4.4 Properties of the seabed

At along-profile I, we determined R at 21 locations over 43.5 km starting when the ice is grounded. Due to the directionality of the detonating cord used as seismic source, we determined R within 32% accuracy at 11 of the 21 shots, where R could not be calibrated against the ice–seawater transition of the ice shelf. At these places, uncertainty, we use the trend or of the magnitude and polarity of R for interpretation rather than the actual value.

At all the places where the ice–seawater contrast is not abrupt, the propagating p-wave, traveling from the ice shelf into the seawater, encounters a series of transmissions and reflections rather than a single transmission. The total amplitude loss over such a stratified ice–seawater contrast is probably larger then our assumed transition of Equation 6. At these place we most likely underestimate R_{s-b}.

While still grounded, we see an increase in R_{i-b} from 0.16 to 0.41 over a 3.9 km distance. As we find it less likely that the subglacial material changes drastically over this short along-flow interval and the acoustic impedance Z of the ice is constant, we attribute this steady increase in acoustic impedance of the subglacial material potentially to increasing compaction, as has been observed by Christianson et al. (2013). We interpret the bed of the grounded ice thus as subglacial till.

Once the ice passed the GL at SP 26, the ~~uncoupled ice stays in contact with~~ floating ice stays close to its flat base down to SP 44 when the seabed starts to descend steeply. The seabed ~~of the ocean cavity (~~downstream, of SP 44 ~~)~~ consists of two distinguishable environments. At interval 2, close to the GL, we have ~~a~~ an 8 km long, and 200 m thick ~~stratified and disturbed sequence~~ sequence with chaotic reflections that changes into ~~an undisturbed less stratified seabed at interval~~ a stratified sequence with semiparallel, reflections at intervals 3 and 4. The ~~disturbed stratified sequence~~ sequence with chaotic reflections close to the GL, having smaller values for R_{s-b}, consists of softer, more porous material then the ~~undisturbed, less stratified seabed. We interpret this disturbed stratified sequence of the second interval as grounding line deposits consisting of subglacial terrestrial sediments~~stratified sequence with semiparallel, reflections. The softness ~~of the seabed~~ is confirmed by the occasionally negative polarity at the steeper downslope of the seabed. ~~The undisturbed, less stratified seabed,~~ We interpret the sequence as an unconsolidated sedimentary sequence.

The stratified sequence with semiparallel, reflections generally has higher values for R_{s-b}, indicating a harder material. This is particularly clear in interval 3, where $0.23 \leq R_{s-b} \leq 0.30$. The seabed structure representative for this second type of environment is most clearly visible between SP 146 and 161, where the flat featureless and abrupt ice–sea contact does not influence the seabed ~~topography~~morphology. In interval 4 we calculated lower values for R_{s-b} but these low values all have a stratified ice–seawater contact above them and so the amplitude loss at the ice–sea transition may be larger then is accounted for ~~. The stratified contact probably causes a larger energy loss than the assumed abrupt ice–seawater transition of Equation 6 accounts for~~ and probably underestimates R_{s-b}. Based on $R_{s-b} \approx 0.31$, we ~~believe we are dealing with~~ interpret them as consolidated sediments but can not exclude bedrock. In any case, this part of the ~~seafloor~~ seabed has properties of an eroded surface, where softer deposits are missing. It could have been created during periods of higher ice-dynamic activity, e.g. during one or several advances of SFG during the last glacial into LGM positions of maximum advance.

4.4 ~~The~~ Characteristics of the subglacial ~~hydrological interpretation~~ feature

~~The landform and basal channel lie~~ At profile I, below the grounded ice between SP 11 and 17, we see the subglacial feature. If this seismic event is from nadir, it would be a separate, 1200 m long and approximately 50 m high, subglacial feature on a hard bed, its dimensions represented by the red semi-circle in Fig. 7. The reflection coefficient $R_{i-b} = -0.04$ represents an ice–unconsolidated, water saturated sediments contact so most likely the subglacial feature would be subglacial conduit on a hard flat bed. A 50 m high conduit would show up in the profiles 5 and 6 but both radar profiles 5 and 6 show a flat base at nadir. We also do not see any evidence of any other subglacial channel entering the ocean cavity on the western side ~~at the western shear margin~~ of SFG. ~~From the radar profiles we can track the landform at least 7.7 km upstream of the GL up to radar profile 3. The landform consists of sediments having some degree of consolidation on its eastern side, but may have a hard rock core as suggested by ?.The ocean cavity close to the GL and downstream of~~

A more likely interpretation is that the subglacial feature is from off-nadir and represents the top of the subglacial channel connecting to the basal channel Fig. 5. The spherically spreading wave front from the off nadir reflections of the subglacial channel arrive before the nadir bed reflections (Fig. 7). When the subglacial channel reaches the dimension of profile 6 this is probably the case. We interpret the subglacial feature as the top of the ~~landform, has a 200 m thick soft stratified, disturbed~~

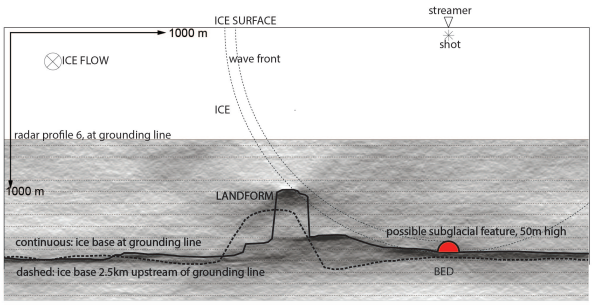

Figure 7. Cross section of the seismic recording geometry of profile I during SP 11 to 17 when the subglacial feature was recorded. The shooting and ice-flow direction are into the page, perpendicular to the cross section. The continuous and dashed black lines represent the ice base at the GL (continuous, profile 6), and 2 km upstream (dashed, profile 5) from the GL. The subglacial feature can either be at nadir in which case its dimensions are represented by the red semicircle or the feature can be off-nadir in which case the feature likely represents the top of the subglacial channel from profile 6. The spherical wave front (dashed quarter circle) shows the off-nadir reflections from the top the basal channel (profile 6) arrive just before the nadir flat bed reflections (so when no semicircle would be present).

~~sedimentation sequence. Sub-shelf noble gas samples (Huhn et al., 2018) suggest subglacial water influx at SFG and modeling of subglacial water routing places the water influx~~ ~280 m subglacial channel approaching the GL.

4.5 The subglacial hydrological interpretation

Our subglacial drainage model predicts a significant ($190 \times 10^3 m^3 a^{-1}$) freshwater influx on the western side of the ice shelf of SFG (Fig.1b). At the grounded ice of SFG profiles 3, 4, 5 and 6 show a subglacial channel connecting to the basal channel at the grounding line. Over a length of 7 km approaching the GL the subglacial channel increases its size from hardly distinguishable from the bed to a 280 m height at the grounding line. The increase in size, when approaching the grounding line, is likely caused by the ocean interacting with the subglacial channel due to tidal motion, thereby melting the channel walls, as suggested by Drews et al. (2017), Horgan et al. (2013) and modeled by Walker et al. (2013). Once passed the grounding line this wide opening of the subglacial channel adjusts to hydrostatic equilibrium and forms the basal and surface channel in which the subglacial drainage water incises. This setting is similar to the subglacial estuary described by Horgan et al. (2013). Because the subglacial channel connects to the only basal channel at the western ~~and eastern sides of SFG. Taking the evidence together we conclude the landform is hosting the transport of sediments that are deposited in the ocean cavity close to~~ side of the ~~GL. Coming back to the classification of surface channels by Alley et al. (2016), we are dealing with a type (2) surface channel ; a subglacially sourced channel (the landform) that intersects with the GL and coincides with modeled subglacial water drainage~~ ice shelf, and because we have a large subglacial drainage influx modeled at the western side of the ice shelf, we interpret the subglacial channel to be a subglacial drainage channel. ~~Basal channels do often form in shear margins (Alley et al., 2019) and the location of this basal channel coincides with the western shear margin of SFG but it is the landform that initiates this basal~~

~~channel. Possibly, shear margins facilitate the formation of landforms hosting the subglacial transport of sediments by water routing.~~

~~What may seem surprising is that we see a much thicker stratified sediment sequence at along-profile I than at along-profile II, which suggests the subglacial drainage is closer to along-profile I. This is not necessarily the case, as along-profile II starts 3.5 km downstream of the GL so~~ The grounded part of profile I consists of a sediment layer and, judging by its reflectivity, becoming more consolidated closer to the grounding line. So the drainage channel probably travels over a layer of subglacial sediments with varying consolidation. The exact nature of the subglacial drainage system we do not know but the radar and seismic profiles do suggest channelized flow close to the grounding line. Possibly we are dealing with a channel that, upstream and outside the survey area, is coupled to a surrounding distributed system as described by Hewitt (2011). Close to the grounding line channelized flow is favorable which corresponds to our observations.

Profile I (1.5 km east of the basal channel) shows an 8 km long and ~200 m thick sedimentary sequence with chaotic reflections just downstream of the GL. Profile III, crossing this sedimentary sequence with chaotic reflections, shows this sequence is 3.5 km wide and only present under the basal channel. Both on the far eastern and western side of profile III there is hardly any structure in the ~~seabed structure at the GL. What we do see is more stratification in all across-profiles below the sub-shelf channel than outside of it and that this stratification extends to the eastern side of across-profile III . Keeping in mind that the off-nadir reflection of the subglacial drainage feature comes from its eastern wall of the landform, we conclude the landform hosts subglacial drainage on its eastern side that caused the disturbed stratified sedimentation sequence at the GL of along-profile I~~ seabed except right under the channel. This sedimentation has most likely been transported by the subglacial drainage channel and consists of unconsolidated, probably subglacial terrestrial sediments. Based on profile I and III we interpret the sedimentation to be point sourced (the subglacial drainage channel) and fan shaped forming a grounding line fan (Powell, 1990) or an ice-proximal fan (Batchelor and Dowdeswell, 2015). This explains the chaotic reflections in this sedimentary sequence and this material being softer as the further downstream part of the sea bed.

~~At radar profiles 1 and 2 the landform can no longer be identified. However, if we follow the flow line upstream connecting the basal channeland landform (the red line in Fig. 1a and d), it connects to an elongated ice surface feature visible in the REMA data (Howat et al., 2019). We do not have radar data to confirm the shape of the bed but we hypothesize that the landform continues further upstream here. If this is indeed the case, the question arises why the landform can not be tracked at radar profiles 9 and 10. Our speculation~~ What is unusual here is that the ~~landform is present at radar profiles 9 and 10 but buried in subglacial material, transported by a subglacial channelized system. As such the landform cannot be detected by the airborne radar profiles 9 and 10.~~ fan has formed under the ice shelf of SFG, a region without surface melt which is a characteristic of fans (Powell and Alley, 2013). But we do have evidence for channelized flow at the grounding line, a noble gas sample suggesting freshwater observation influx of terrestrial origin likely (Huhn et al., 2018) and a significant modeled channelized freshwater influx on the western side of SFG confirmed by the presence of a single basal channel on the western side. We also have an unusual ocean cavity with a steeply descending seabed and a stable grounding line. These are typical conditions for the formation of a fan at the grounding line (Powell, 1990; Powell and Alley, 2013; Batchelor and Dowdeswell, 2015).

5 Conclusions

We investigated the characteristics of a subglacial channel continuing as a basal channel across the grounding line of the Support Force Glacier. ~~Our observations do confirm~~ As this is the only subglacial channel, basal channel system on the western side of Support Force Glacier subglacial drainage takes place through channelized flow close to the grounding line. Our observations concur with the categorization of Alley et al. (2019), i.e. ~~the basal channel conincides with the western shear margin. However, rather than the channel being formed by the surface depression in the shear zone of the grounded ice and adjusting to the hydrostatic equilibrium once the ice is afloat, we find that the channel originates at a subglacial landform, which agrees ? . On its eastern side the landform consists of sediments, but we cannot conclude whether a deeper hard rock core is also present~~subglacially sourced channels that intersect the grounding line and coincide with modeled subglacial water drainage. We find no evidence for the hypothesis the basal channel is initially formed by a landform as suggested by Jeofry et al. (2018b) . The increase in channel height close to the grounding line is probably caused by the ocean interacting with the subglacial channel thereby increasing its height as suggested by Horgan et al. (2013) and Walker et al. (2013).

~~The landform hosts a channelized subglacial drainage, which transports sediments downstream. These are deposited just seaward of~~ In seismic profiles I and III at the seabed, close to the grounding line, ~~where we identified a~~ we identify an 8 km long, 3.5 km wide and 200 m thick~~soft, disturbed, stratified sedimentation sequence at the seafloor.~~ , soft, sedimentary sequence with chaotic reflections that most likely have been deposited by the subglacial channel. This makes the 200 m sedimentary sequence point sourced and fan shaped and so we interpret this sequence as a grounding line fan which is unusual for ice shelves.

Further downstream the ~~seafloor~~ seabed consists of harder, ~~undisturbed and less~~ stratified consolidated sediments with semiparallel reflections, possibly also bedrock. We attribute these two units to originate from different development phases: whereas the harder sequence is potentially a left-over from a farther advanced grounding line, e.g. coming along with stronger erosion during advances into the LGM, the softer sediment sequence seems to be the result of comparatively recent post-LGM and Holocene grounding line depositions.

Apart from the basal channel and individual ~~anticlines~~concave cavities, the base of the ice shelf downstream of the grounding line is relatively flat~~and almost horizontal~~, indicating that basal melt rates are relatively low. We attribute the observed widening of the basal channel to melting along its flanks, which we also observe at the flanks of ~~anticlines~~ concave cavities in the ice shelf base. The melting increases further in downstream direction. To date it is unlikely that warmer water is already in the cavity near the grounding line. But even if it ~~was~~were, the geometry of the steeply descending ~~seafloor~~ seabed downstream of the grounding line would limit the direct contact of potentially warmer water with the ice shelf base, thus limiting basal melt rates, unless the cavity was fully flooded with warmer water. This is in contrast to the typically envisaged geometry and ice–ocean interaction at grounding lines, which often envisage a steeply rising ice shelf base just downstream of grounding lines, where circulation is dominated by the ice pump mechanism. With our improved ~~characterisation~~ characterization of the grounding line area of SFG, future ~~modelling~~ modeling studies should investigate how ~~this area might react differently~~ differently this region

might react to the presence of warm deep water in the cavity than for instance the glaciers in the Amundsen Sea Embayment region and thus quantify the role of the ~~seafloor~~ seabed geometry.

Acknowledgements. The Filchner Ice Shelf Project (FISP) was funded by the AWI Strategy Fund. The Grounding Line Location (GLL) product was provided by DLR via ESA CCI Antarctic Ice Sheet. Hugh Corr was supported by the UK Natural Environment Research Council large grant "Ice shelves in a warming world: Filchner Ice Shelf System" (NE/L013770/1). Some data used in this study were acquired by NASA's Operation IceBridge. TerraSAR-X data used for grounding line detection and surface velocities were made available through DLR proposal HYD2059. Niklas Neckel received funding from the European Union's Horizon 2020 research and innovation program under grant agreement No 689443 via project iCUPE (Integrative and Comprehensive Understanding on Polar Environments).We thank the field guides Dave Routledge and Bradley Morrell for their unwavering guidance and support. We also thank BAS for their logistic support and hospitality. A special thanks goes to the pilots delivering the hardware at the right time at the right remote place. Without them, this survey would have been impossible.

References

Ainslie, M. A. and McColm, J. G.: A simplified formula for viscous and chemical absorption in sea water, The Journal of the Acoustical Society of America, 103, 1671–1672, https://doi.org/10.1121/1.421258, https://doi.org/10.1121/1.421258, 1998.

Aki, K. and Richards, P. G.: Quantitative Seismology, University Science Books, 2 edn., http://www.amazon.com/exec/obidos/redirect?tag=citeulike07-20&path=ASIN/0935702962, 2002.

Alley, K. E., Scambos, T. A., Siegfried, M. R., and Fricker, H. A.: Impacts of warm water on Antarctic ice shelf stability through basal channel formation, Nature Geoscience, 9, 290 EP –, https://doi.org/10.1038/ngeo2675, 2016.

Alley, K. E., Scambos, T. A., Alley, R. B., and Holschuh, N.: Troughs developed in ice-stream shear margins precondition ice shelves for ocean-driven breakup, Science Advances, 5, eaax2215, https://doi.org/10.1126/sciadv.aax2215, http://advances.sciencemag.org/content/5/10/eaax2215.abstract, 2019.

Batchelor, C. and Dowdeswell, J.: Ice-sheet grounding-zone wedges (GZWs) on high-latitude continental margins, Marine Geology, 363, 65 – 92, https://doi.org/https://doi.org/10.1016/j.margeo.2015.02.001, http://www.sciencedirect.com/science/article/pii/S0025322715000304, 2015.

Beaud, F., Flowers, G. E., and Venditti, J. G.: Modeling Sediment Transport in Ice-Walled Subglacial Channels and Its Implications for Esker Formation and Proglacial Sediment Yields, Journal of Geophysical Research: Earth Surface, 123, 3206–3227, https://doi.org/10.1029/2018JF004779, https://agupubs.onlinelibrary.wiley.com/doi/abs/10.1029/2018JF004779, 2018.

Bentley, C. R. and Kohnen, H.: Seismic refraction measurements of internal friction in Antarctic ice, , 81, 1519–1526, 1976.

Bindschadler, R., Choi, H., Wichlacz, A., Bingham, R., Bohlander, J., Brunt, K., Corr, H., Drews, R., Fricker, H., Hall, M., Hindmarsh, R., Kohler, J., Padman, L., Rack, W., Rotschky, G., Urbini, S., Vornberger, P., and Young, N.: Getting around Antarctica: new high-resolution mappings of the grounded and freely-floating boundaries of the Antarctic ice sheet created for the International Polar Year, The Cryosphere, 5, 569–588, https://doi.org/10.5194/tc-5-569-2011, https://www.the-cryosphere.net/5/569/2011/, 2011.

Bingham, R. G., Siegert, M. J., Young, D. A., and Blankenship, D. D.: Organized flow from the South Pole to the Filchner-Ronne ice shelf: An assessment of balance velocities in interior East Antarctica using radio echo sounding data, Journal of Geophysical Research: Earth Surface, 112, https://doi.org/10.1029/2006JF000556, https://agupubs.onlinelibrary.wiley.com/doi/abs/10.1029/2006JF000556, 2007.

Christianson, K., Parizek, B. R., Alley, R. B., Horgan, H. J., Jacobel, R. W., Anandakrishnan, S., Keisling, B. A., Craig, B. D., and Muto, A.: Ice sheet grounding zone stabilization due to till compaction, Geophysical Research Letters, 40, 5406–5411, https://doi.org/10.1002/2013GL057447, https://agupubs.onlinelibrary.wiley.com/doi/abs/10.1002/2013GL057447, 2013.

Christianson, K., Peters, L. E., Alley, R. B., Anandakrishnan, S., Jacobel, R. W., Riverman, K. L., Muto, A., and Keisling, B. A.: Dilatant till facilitates ice-stream flow in northeast Greenland, Earth and Planetary Science Letters, 401, 57–69, https://doi.org/10.1016/j.epsl.2014.05.060, 2014.

Dow, C. F., Lee, W. S., Greenbaum, J. S., Greene, C. A., Blankenship, D. D., Poinar, K., Forrest, A. L., Young, D. A., and Zappa, C. J.: Basal channels drive active surface hydrology and transverse ice shelf fracture, Science Advances, 4, https://doi.org/10.1126/sciadv.aao7212, https://advances.sciencemag.org/content/4/6/eaao7212, 2018.

Drews, R.: Evolution of ice-shelf channels in Antarctic ice shelves, The Cryosphere, 9, 1169–1181, https://doi.org/10.5194/tc-9-1169-2015, https://www.the-cryosphere.net/9/1169/2015/, 2015.

Drews, R., Pattyn, F., Hewitt, I. J., Ng, F. S. L., Berger, S., Matsuoka, K., Helm, V., Bergeot, N., Favier, L., and Neckel, N.: Actively evolving subglacial conduits and eskers initiate ice shelf channels at an Antarctic grounding line, Nature Communications, 8, 15 228, https://doi.org/10.1038/ncomms15228, https://doi.org/10.1038/ncomms15228, 2017.

Dutrieux, P., Vaughan, D. G., Corr, H. F. J., Jenkins, A., Holland, P. R., Joughin, I., and Fleming, A. H.: Pine Island glacier ice shelf melt distributed at kilometre scales, The Cryosphere, 7, 1543–1555, https://doi.org/10.5194/tc-7-1543-2013, https://www.the-cryosphere.net/7/1543/2013/, 2013.

Dutrieux, P., Stewart, C., Jenkins, A., Nicholls, K. W., Corr, H. F. J., Rignot, E., and Steffen, K.: Basal terraces on melting ice shelves, Geophysical Research Letters, 41, 5506–5513, https://doi.org/10.1002/2014GL060618, https://agupubs.onlinelibrary.wiley.com/doi/abs/10.1002/2014GL060618, 2014.

Fahnestock, M., Scambos, T., Moon, T., Gardner, A., Haran, T., and Klinger, M.: Rapid large-area mapping of ice flow using Landsat 8, Remote Sensing of Environment, 185, 84 – 94, https://doi.org/10.1016/j.rse.2015.11.023, http://www.sciencedirect.com/science/article/pii/S003442571530211X, landsat 8 Science Results, 2016.

Fretwell, P., Pritchard, H. D., Vaughan, D. G., Bamber, J. L., Barrand, N. E., Bell, R., Bianchi, C., Bingham, R. G., Blankenship, D. D., Casassa, G., Catania, G., Callens, D., Conway, H., Cook, A. J., Corr, H. F. J., Damaske, D., Damm, V., Ferraccioli, F., Forsberg, R., Fujita, S., Gim, Y., Gogineni, P., Griggs, J. A., Hindmarsh, R. C. A., Holmlund, P., Holt, J. W., Jacobel, R. W., Jenkins, A., Jokat, W., Jordan, T., King, E. C., Kohler, J., Krabill, W., Riger-Kusk, M., Langley, K. A., Leitchenkov, G., Leuschen, C., Luyendyk, B. P., Matsuoka, K., Mouginot, J., Nitsche, F. O., Nogi, Y., Nost, O. A., Popov, S. V., Rignot, E., Rippin, D. M., Rivera, A., Roberts, J., Ross, N., Siegert, M. J., Smith, A. M., Steinhage, D., Studinger, M., Sun, B., Tinto, B. K., Welch, B. C., Wilson, D., Young, D. A., Xiangbin, C., and Zirizzotti, A.: Bedmap2: improved ice bed, surface and thickness datasets for Antarctica, The Cryosphere, 7, 375–393, https://doi.org/10.5194/tc-7-375-2013, https://www.the-cryosphere.net/7/375/2013/, 2013.

Fürst, J. J., Durand, G., Gillet-Chaulet, F., Tavard, L., Rankl, M., Braun, M., and Gagliardini, O.: The safety band of Antarctic ice shelves, Nature Climate Change, 6, 479–482, https://doi.org/10.1038/nclimate2912, https://doi.org/10.1038/nclimate2912, 2016.

Hewitt, I. J.: Modelling distributed and channelized subglacial drainage: the spacing of channels, Journal of Glaciology, 57, 302–314, https://doi.org/10.3189/002214311796405951, 2011.

Holland, C. and Anandakrishnan, S.: Subglacial seismic reflection strategies when source amplitude and medium attenuation are poorly known, J. Glaciol., 55, 931–937, 2009.

Horgan, H., Alley, R., Christianson, K., Jacobel, R., Anandakrishnan, S., Muto, A., Beem, L., and Siegfried, M.: Estuaries beneath ice sheets, Geology, 41, textit[in press], https://doi.org/10.1130/G34654.1, 2013.

Howat, I. M., Porter, C., Smith, B. E., Noh, M.-J., and Morin, P.: The Reference Elevation Model of Antarctica, The Cryosphere, 13, 665–674, https://doi.org/10.5194/tc-13-665-2019, https://www.the-cryosphere.net/13/665/2019/, 2019.

Huhn, O., Hattermann, T., Davis, P. E. D., Dunker, E., Hellmer, H. H., Nicholls, K. W., Østerhus, S., Rhein, M., Schröder, M., and Sültenfuß, J.: Basal Melt and Freezing Rates From First Noble Gas Samples Beneath an Ice Shelf, Geophysical Research Letters, 45, 8455–8461, https://doi.org/10.1029/2018GL079706, https://agupubs.onlinelibrary.wiley.com/doi/abs/10.1029/2018GL079706, 2018.

Humbert, A., Steinhage, D., Helm, V., Beyer, S., and Kleiner, T.: Missing Evidence of Widespread Subglacial Lakes at Recovery Glacier, Antarctica, Journal of Geophysical Research: Earth Surface, 123, 2802–2826, https://doi.org/10.1029/2017JF004591, https://agupubs.onlinelibrary.wiley.com/doi/abs/10.1029/2017JF004591, 2018.

Jenkins, A.: Convection-Driven Melting near the Grounding Lines of Ice Shelves and Tidewater Glaciers, J. Phys. Oceanogr, 41, 2279 – 2294, 2011.

Jeofry, H., Ross, N., Corr, H. F. J., Li, J., Morlighem, M., Gogineni, P., and Siegert, M. J.: A new bed elevation model for the Weddell Sea sector of the West Antarctic Ice Sheet, Earth System Science Data, 10, 711–725, https://doi.org/10.5194/essd-10-711-2018, https://www.earth-syst-sci-data.net/10/711/2018/, 2018a.

Jeofry, H., Ross, N., Le Brocq, A., Graham, A. G. C., Li, J., Gogineni, P., Morlighem, M., Jordan, T., and Siegert, M. J.: Hard rock landforms generate 130 km ice shelf channels through water focusing in basal corrugations, Nature Communications, 9, 4576, https://doi.org/10.1038/s41467-018-06679-z, https://doi.org/10.1038/s41467-018-06679-z, 2018b.

Le Brocq, A. M., Ross, N., Griggs, J. A., Bingham, R. G., Corr, H. F. J., Ferraccioli, F., Jenkins, A., Jordan, T. A., Payne, A. J., Rippin, D. M., and Siegert, M. J.: Evidence from ice shelves for channelized meltwater flow beneath the Antarctic Ice Sheet, Nature Geoscience, 6, 945 EP –, https://doi.org/10.1038/ngeo1977, 2013.

Lüttig, C., Neckel, N., and Humbert, A.: A Combined Approach for Filtering Ice Surface Velocity Fields Derived from Remote Sensing Methods, Remote Sensing, 9, https://doi.org/10.3390/rs9101062, https://www.mdpi.com/2072-4292/9/10/1062, 2017.

Marsh, O. J., Fricker, H. A., Siegfried, M. R., Christianson, K., Nicholls, K. W., Corr, H. F. J., and Catania, G.: High basal melting forming a channel at the grounding line of Ross Ice Shelf, Antarctica, Geophysical Research Letters, 43, 250–255, https://doi.org/10.1002/2015GL066612, https://agupubs.onlinelibrary.wiley.com/doi/abs/10.1002/2015GL066612, 2016.

Paden, J., Li, J., Leuschen, C., Rodriguez-Morales, F., and Hale., R.: 2010, updated 2019. IceBridge MCoRDS L2 Ice Thickness, Version 1., Boulder, Colorado USA. NASA National Snow and Ice Data Center Distributed Active Archive Center., https://doi.org/10.5067/GDQ0CUCVTE2Q, 2019.

Peters, L. E., Anandakrishnan, S., Alley, R. B., and Voigt, D. E.: Seismic attenuation in glacial ice: A proxy for englacial temperature, J. Geophys. Res., 117, F02 008, https://doi.org/10.1029/2011JF002201,, 2012.

Powell, R. D.: Glacimarine processes at grounding-line fans and their growth to ice-contact deltas, Geological Society, London, Special Publications, 53, 53–73, https://doi.org/10.1144/GSL.SP.1990.053.01.03, https://sp.lyellcollection.org/content/53/1/53, 1990.

Powell, R. D. and Alley, R. B.: Grounding-Line Systems: Processes, Glaciological Inferences and the Stratigraphic Record, pp. 169–187, American Geophysical Union (AGU), https://doi.org/10.1029/AR071p0169, https://agupubs.onlinelibrary.wiley.com/doi/abs/10.1029/AR071p0169, 2013.

Rignot, E., Mouginot, J., and Scheuchl, B.: Ice Flow of the Antarctic Ice Sheet, Science, 333, 1427–1430, https://doi.org/10.1126/science.1208336, https://science.sciencemag.org/content/333/6048/1427, 2011.

Rippin, D., Bingham, R., Jordan, T., Wright, A., Ross, N., Corr, H., Ferraccioli, F., Brocq, A. L., Rose, K., and Siegert, M.: Basal roughness of the Institute and Möller Ice Streams, West Antarctica: Process determination and landscape interpretation, Geomorphology, 214, 139 – 147, https://doi.org/http://dx.doi.org/10.1016/j.geomorph.2014.01.021, http://www.sciencedirect.com/science/article/pii/S0169555X14000671, 2014.

Scambos, T., Haran, T., Fahnestock, M., Painter, T., and Bohlander, J.: MODIS-based Mosaic of Antarctica (MOA) data sets: Continent-wide surface morphology and snow grain size, Remote Sensing of Environment, 111, 242 – 257, https://doi.org/https://doi.org/10.1016/j.rse.2006.12.020, http://www.sciencedirect.com/science/article/pii/S0034425707002854, remote Sensing of the Cryosphere Special Issue, 2007.

Scambos, T., Fahnestock, M., Moon, T., Gardner, A., and Klinger., M.: Global Land Ice Velocity Extraction from Landsat 8 (GoLIVE), Version 1. Antarctica., Boulder, Colorado USA. NSIDC: National Snow and Ice Data Center., https://doi.org/10.7265 /N5ZP442B, 2016.

Schlegel, R., Diez, A., Löwe, H., Mayer, C., Lambrecht, A., Freitag, J., Miller, H., Hofstede, C., and Eisen, O.: Comparison of elastic moduli from seismic diving-wave and ice-core microstructure analysis in Antarctic polar firn, 60, 220–230, https://doi.org/DOI: 10.1017/aog.2019.10, https://doi.org/10.1017/aog.2019.10, 2019.

Shreve, R. L.: Movement of Water in Glaciers, Journal of Glaciology, 11, 205–214, https://doi.org/10.3189/S002214300002219X, 1972.

Smith, A. M.: Basal conditions on Rutford Ice Stream, West Antarctica, from seismic observations, J. Geophys. Res., 102, 543–552, 1997.

Smith, W. H. F. and Wessel, P.: Gridding with continuous curvature splines in tension, Geophysics, 55, 293–305, 1990.

Strozzi, T., Luckman, A., Murray, T., Wegmuller, U., and Werner, C. L.: Glacier motion estimation using SAR offset-tracking procedures, IEEE Transactions on Geoscience and Remote Sensing, 40, 2384–2391, https://doi.org/10.1109/TGRS.2002.805079, 2002.

Thomas, R. and MacAyeal, D.: Derived Characteristics of the Ross Ice Shelf, Antarctica (Abstract only), Annals of Glaciology, 3, 349–349, https://doi.org/10.3189/S0260305500003220, 1982.

Vaughan, D. G., Corr, H. F. J., Bindschadler, R. A., Dutrieux, P., Gudmundsson, G. H., Jenkins, A., Newman, T., Vornberger, P., and Wingham, D. J.: Subglacial melt channels and fracture in the floating part of Pine Island Glacier, Antarctica, Journal of Geophysical Research: Earth Surface, 117, https://doi.org/10.1029/2012JF002360, https://agupubs.onlinelibrary.wiley.com/doi/abs/10.1029/2012JF002360, 2012.

Walker, R. T., Parizek, B. R., Alley, R. B., Anandakrishnan, S., Riverman, K. L., and Christianson, K.: Ice-shelf tidal flexure and subglacial pressure variations, Earth and Planetary Science Letters, 361, 422 – 428, https://doi.org/https://doi.org/10.1016/j.epsl.2012.11.008, http://www.sciencedirect.com/science/article/pii/S0012821X12006164, 2013.